APPLICATION OF GEOCHEMICAL TRACERS TO DETERMINE THE SOURCES CONTRIBUTING TO RUNOFF AT THE SEMI-ARID WALNUT GULCH EXPERIMENTAL WATERSHED, ARIZONA

by

Laura Elice Nakolan

A Thesis Submitted to the Faculty of the

DEPARTMENT OF HYDROLOGY AND ATMOSPHERIC SCIENCES

In Partial Fulfillment of the Requirements

For the Degree of

MASTER OF SCIENCE
WITH A MAJOR IN HYDROLOGY

In the Graduate College

THE UNIVERSITY OF ARIZONA

2017

STATEMENT BY AUTHOR

The thesis titled *Application of Geochemical Tracers to Determine the Sources Contributing to Runoff at the Semi-Arid Walnut Gulch Experimental Watershed, Arizona* prepared by Laura E. Nakolan has been submitted in partial fulfillment of requirements for a master's degree at the University of Arizona and is deposited in the University Library to be made available to borrowers under rules of the Library.

Brief quotations from this thesis are allowable without special permission, provided that an accurate acknowledgement of the source is made. Requests for permission for extended quotation from or reproduction of this manuscript in whole or in part may be granted by the head of the major department or the Dean of the Graduate College when in his or her judgment the proposed use of the material is in the interests of scholarship. In all other instances, however, permission must be obtained from the author.

SIGNED: Laura E. Nakolan

APPROVAL BY THESIS DIRECTOR

This thesis has been approved on the date shown below:

Dr. Peter A. Troch
Professor of Hydrology and Atmospheric Sciences

May 3rd, 2017
Date

ACKNOWLEDGEMENTS

To my family and friends: thank you for being a constant source of support, love and encouragement in every aspect of my life. Thank you also to my advising committee for giving me valuable insight on my project, for your kindness and for your flexibility with my schedule and living situation. Finally, thank you to the staff of the University of Arizona Hydrology Department for being a constant source of inspiration to me, and for fostering my excitement about hydrology through exciting and interesting lectures, homework assignments, labs, projects and field trips.

TABLE OF CONTENTS

LIST OF FIGURES

LIST OF FIGURES (CONTINUED)

LIST OF TABLES

ABSTRACT

Prior observations by Koch (2005) suggest the presence of soil water mixed with current rainfall in runoff samples at the Kendall subwatershed of the USDA-Agricultural Research Service Walnut Gulch Experimental Watershed (WGEW). However, previous observations elsewhere in the WGEW have shown runoff to consist mainly of current precipitation (Goodrich et al., 2004). The disparity between the two studies demonstrates a need for continued research; therefore, this study uses isotope and solute geochemical tracers to determine the sources contributing to runoff at the Lucky Hills subwatershed of the WGEW during the 2015 monsoon season. A comparison of the stable isotopes of water (^{2}H and ^{18}O) in runoff to those in precipitation and soil water, shows that runoff and precipitation are distinct ($p < 0.05$), while soil water cannot be differentiated from runoff ($p > 0.05$). However, graphical representations of chloride and sulfate concentrations in the three water sources (precipitation, soil water and runoff), conclusively reveal that there is negligible soil water present in the runoff at Lucky Hills. Therefore, it is likely that there is no soil water mixing into the runoff at the Lucky Hills subwatershed, but more research is necessary to confirm these results. Because no runoff or soil water data was generated at the Kendall subwatershed during the 2015 monsoon season, continued research is necessary to draw conclusions about the sources contributing to runoff in the Kendall subwatershed, and in other portions of the Walnut Gulch Experimental Watershed.

1. INTRODUCTION

Establishing a clear understanding of storm runoff generation, its timing, and mixing dynamics is essential to make realistic catchment conceptualizations and models (Hrachowitz et al., 2013). Runoff modeling allows scientists to determine the conditions under which runoff is generated, where it comes from, in what quantities and under what water quality conditions, which can positively impact the way we make decisions about water use, vegetation and land use changes (Hundecha and Bardossy, 2004), soil erosion, and non-point source pollution management (Maneta et al., 2008; Fitzjohn et al., 1997). However, the spatial and temporal variability of soil properties, soil moisture and precipitation in nature make runoff generation a highly complex process at the catchment scale (Smith and Hebbert, 1979; Robinson and Sivapalan, 1995; McGlynn and McDonnell, 2003). Due to these complications, runoff generation is still not entirely understood, and more research is required to further our knowledge in the field.

Arid and semi-arid climates present particular challenges to storm runoff generation research. Due to the variability in time and space of storm intensity and duration and the ephemeral nature of streams, runoff events and data collection can be irregular, creating a deficit in accurate data to be used in rainfall-runoff modeling (Yair and Lavee, 1985). In addition to limited data collection, Pilgrim et al. (1988) list other issues affecting streamflow data quality in semi-arid environments: “isolation of gauging stations in low density populations; difficulty of access in rainy periods; lack of suitable natural control sections in streams with movable beds, and high cost of artificial controls; and difficulty of current metering with high sediment and debris loads.” Understandably, runoff generation and hydrologic processes are less understood in these complicated environments; however, effective water management is only made possible by

gaining an understanding of the hydrologic processes occurring in a region. In arid and semi-arid regions, which experience population growth despite the limited resources, recent droughts and global warming (Ragab and Prudhomme, 2002; Arnell, 1999; Arnell, 2004), continued research is essential.

In semi-arid climates and in general, when considering the interaction of water sources during runoff generation, it is important to be able to tell the water sources apart. Rainfall, river, lake and soil water are made isotopically distinguishable by the evaporative effects imparted on them by the dry air (Ingraham et al., 1998), causing the stable isotopes of water (^{2}H and ^{18}O) to be valuable geochemical tracers in hydrology research. Concentrations of solutes commonly found in water, such as chloride and sulfate, are also useful geochemical tracers due to the natural and unique mineral dissolution that occurs from the soil, allowing soil water to be differentiated from precipitation (Pearce et al., 1986), and for groundwater aquifer systems to be distinguished (Robertson, 1989; Robertson, 1992). Both isotope and solute tracers have been used in a wide range of environments to track the movement of water in the subsurface; however, owing to the importance of groundwater as the primary water resource used to sustain life in arid and semi-arid environments, subsurface hydrology in these environments is generally analyzed in the context of groundwater replenishment (Allison and Hughes, 1983; Wood and Sanford, 1995; Allison et al., 1985; Allison et al., 1994). While geochemical tracers have been applied to humid environments to study rainfall-runoff generation involving subsurface flow (McGuire et al., 2006; Brammer, 1996; Luxmoore, 1990; Peters and Ratcliffe, 1998; McDonnell et al., 1991), it is common in semi-arid environments to assume little to no interaction between soil water and runoff (Yair and Lavee, 1985; Puigdefabregas et al., 1998; Baillie et al., 2007).

Precipitation and runoff data collected by Goodrich et al. (2004) at the semi-arid Walnut Gulch Experimental Watershed (WGEW) in southeastern Arizona show similar isotope values, suggesting little to no soil water interaction with runoff. These observations have led to assumptions about the interchangeability of precipitation and runoff samples at Walnut Gulch when considering stable isotope values (Baillie et al., 2007). However, observations by Koch (2005) indicate that this assumption may not be valid for all subwatersheds within Walnut Gulch. Koch saw similar isotope values in precipitation and runoff at the Lucky Hills subwatershed, but found the runoff at the Kendall subwatershed to be more depleted in ^{18}O and D than precipitation, which he hypothesized might be due to the flushing of stored soil water during storms as a result of pressure wave translator flow (Weiler and McDonnell, 2004) and mesopore or perched-aquifer flow (Wilson et al., 1991). Studies at the semi-arid Dehesas catchment in Spain also warn that subsurface stormflow cannot be ignored (Maneta et al., 2008; Schaik et al., 2008; Schaik et al., 2014).

Interactions between soil water and runoff at the WGEW could challenge existing assumptions about rainfall-runoff generation at Walnut Gulch and in general in arid and semi-arid catchments. Therefore, in order to clarify and gain more insight into the conflicting observations seen by Goodrich et al. (2004) and Koch (2005), the goals of this study were to use isotope and solute geochemical tracers found in precipitation, soil water and runoff, to ascertain the source composition of runoff at the Kendall and Lucky Hills subwatersheds of the WGEW.

2. METHODS

Site Description

The Walnut Gulch Experimental Watershed (WGEW), operated since the 1950's by the USDA-Agricultural Research Service (ARS), is a popular research site for hydrology and environmental processes in semi-arid environments. It is located in the Upper San Pedro River Basin in southeastern Arizona, U.S.A. (Figure 1). The 150 km^2 watershed is ideal for field studies in semi-arid environments because it is well equipped to record precipitation, runoff, and sediment transport, as well as meteorologic and soil moisture conditions with its expansive network of instrumentation (Figure 2). The WGEW is located in a transition zone between the Chihuahuan and Sonoran Deserts, with elevations ranging from 1250 to 1585 meters AMSL (Renard et al., 1993). Its subwatersheds encompass a range of precipitation, soil and vegetation conditions, which have been well studied since the inception of the WGEW research facility.

The WGEW receives an average of 312 mm of precipitation annually, approximately 60% of which occurs during the summer (July, August and September) as a result of the North American Monsoon (Goodrich et al., 2008). However, inter-annual variability is large. According to Goodrich et al. (2008), the WGEW has experienced annual precipitation totals ranging from 165 mm (1965) to 525 mm (1983). Summer precipitation is typically a result of convective thunderstorms, which result in short-duration, high-intensity precipitation events with limited areal extent (Osborn and Reynolds, 1963). The remaining 40% of the precipitation is a result of low intensity frontal systems in the winter (December to March), and relatively rare tropical depressions originating in the Gulf of Mexico, most common in September and October (Gochis et al., 2006). The streams at the WGEW are ephemeral, and runoff generation almost exclusively occurs during in the summer during high-intensity monsoon storms (Goodrich et al.,

2008). As a result of plant transpiration and bare soil evaporation during the summer, deep root zone infiltration (greater than ~0.3 m) is insignificant in the hot summer, although it can occur during the low-intensity winter storms (Scott et al., 2000).

Located primarily in a high foothill alluvial fan portion of the San Pedro Basin, the geology of the WGEW is mostly Cenozoic alluvium (Gleeson Road Conglomerate) consisting of clastic materials that sit deep (> 400 m) below the soil surface (Figure 3). This alluvial fill forms a large groundwater reservoir, with water table depths ranging from 50 to 145 meters in the lower to central parts of the watershed, respectively (Renard et al., 1993). The southern and southeastern portions of the WGEW, not studied in this paper, also contain volcanic and igneous-intrusive rocks due to a history of tectonism in the area. The current research focuses on the Lucky Hills and Kendall unit source watersheds within the WGEW, the vegetal and soil properties of which are distinct (Figures 4 and 5, respectively).

Lucky Hills

The Lucky Hills subwatershed is located in the lower basin of the larger WGEW. Its vegetation primarily consists of shrub type species, including creosote (*Larrea tridentate*), white-thorn (*Acacia constricta*), tarbush (*Flourensia cernua*), snakeweed (*Gutierrezia sarothrae*), and burroweed (*Aplopappus tenuisectus*) (Renard et al., 1993). The soils at Lucky Hills are part of the Lucky Hills-McNeal Group, which tend to be of poorly to moderately permeable sandy and gravelly loams (Breckenfeld et al., 1995), and which sit above a soft caliche layer (located one foot or more below the soil surface) (Kincaid et al., 1964). The soils of the Lucky Hills-McNeal Group are often immature due to frequent erosion during high intensity storms (Breckenfeld et al., 1995).

Kendall

The Kendall subwatershed is located in the upper basin, which is higher in elevation and is dominated by grass species of black grama (*Bouteloua eriopoda*), blue grama (*B. gracilis*), sideoats grama (*B. curtipendula*), bush muhly (*Muhlenbergia porter*), and Lehmann lovegrass (*Eragrostis lehmanniana*) (Renard et al., 1993). The soil at Kendall is part of the Elgin-Stronghold Group, typically containing deep sandy gravel loams formed on beds of conglomerate (Breckenfeld et al., 1995). These soils are more permeable than those of Lucky Hills and do not contain a caliche layer, allowing rainfall to abruptly penetrate to considerable depths and the soil to remain moist for long durations of time (Kincaid et al., 1964).

Sample Collection

In order to determine the source composition of the runoff, samples of precipitation, soil water and runoff water were collected at the WGEW (Figure 1). Precipitation samples were collected during the 2015 summer monsoon season at both the Lucky Hills and Kendall subwatersheds (Figure 2). However, the 2015 monsoon season was relatively dry, and unfortunately there was not enough precipitation over the Kendall 112 subwatershed (1.86 hectares) to produce soil water and runoff samples. Therefore, the analysis of runoff composition will focus on solely the Lucky Hills subwatershed. However, analyses based on precipitation only, such as the isotopic variability in rainfall spatially across each subwatershed and between the two subwatersheds are presented for both Lucky Hills and Kendall.

Precipitation

Precipitation was collected as it fell during storm events, and retrieved from the collectors the following morning. Rainfall sampling locations were chosen to address spatial variability in the watersheds. Three of the five collecting locations were placed next to three preexisting recording rain gauges at or near the site, which allowed us to track the storm direction and intensity associated with samples. The other two collecting locations were placed at non-recording rain gauges within the watershed.

Ten collectors were used to collect precipitation samples at Lucky Hills (Figure 6, yellow). In order to determine sample variability, two rain collectors were placed adjacent to each other at three of the five sites (RG-P105, RG-384, RG-083). Precipitation samples were collected by funneling water into ~1 liter glass mason jars. When deployed, clean jars were supplied with a thin layer of mineral oil in order to prevent isotopic evaporative enrichment (Scholl et al., 1996). Site RG-083 housed two additional collectors that did not use mineral oil, in order to test the effects of mineral oil on isotopic fractionation related to evaporation.

The morning following each rainstorm, aliquots from each jar were transferred to 4ml glass vials with polyseal caps as follows: without shaking the mason jar and mineral oil, a clean pipette was partially filled with air and inserted half way into the sample; the air was gently released from the pipette in order to attempt to shake off any mineral oil lingering to the pipette; the sample was collected into the pipette and gently removed from the water in the mason jar. The pipette was wiped with a paper towel in order to remove the mineral oil that attached itself to the exiting pipette, a small amount of sample was flushed out, and finally the sample was deposited into the 4ml vial with minimal contact between the pipette and vial. Precipitation samples were stored at room temperature in the dark until analysis.

Soil Water

Soil water was collected in the streambed using four Soilmoisture Pressure/Vacuum Soil Water, 24", 2 bar suction lysimeters (Figure 7). Two lysimeters each were placed 9.1 and 21.3 meters (30 and 70 feet) upstream of the runoff collection site, at 40 and 60 centimeter depths. Soil water samples were labelled with respect to their collection type (suction lysimeter, "LY"), and the suction lysimeter's location and depth. Therefore, a soil water sample collected from the suction lysimeter that is 21.3 meters upstream of Flume-103 and 40cm below the soil surface would be labelled "LY-21m40cm". Daily attempts were made to extract soil water samples from the lysimeters, although they did not always produce a sample due to insufficient soil moisture. To collect the samples, a hand pump was used to apply suction of ~345 kPa (~50 psi) to the lysimeters for 1-2 hours. The same hand pump was then used to pump any accumulated water in the lysimeters directly into 4ml glass vials with polyseal caps. Soil water samples were stored at room temperature in the dark.

Soil Samples

Daily soil sample collection was added to the experimental design in late July 2015 to provide continuous soil water data, since suction lysimeters will not produce soil water samples at low soil moisture conditions. Soil sample collection was also added to the experimental design in order to address concerns about the omission of immobile water, the water in micropores or tightly-bound films around a soil particle, which suction lysimeter struggle to extract (Landon et al., 1999).

Samples were collected using a hand auger to dig a hole close to each lysimeter pair approximately 60 centimeters deep, and samples were collected from the sides of the hole at 2, 5, 10, 20, 40 and 60 centimeter depths. The samples were collected directly into 4ml glass vials with polyseal caps and immediately transferred to a cooler after collection. The samples were placed in a refrigerator while awaiting analysis.

Runoff

Runoff was collected at Flume 103 in the Lucky Hills watershed 103 (3.68 hectares) by two methods of collection: an ISCO automated water sampling device, and an automated traversing slot sediment sampler already operated at the site by the Southwest Watershed Research Center (USDA-ARS) since 1977 (Nichols et al., 2008). The sediment sampler was triggered to collect every three to five minutes after the water level in a stilling well was raised by more than seven centimeters. Sample collection on the ISCO autosampler was programmed to begin when the water level raised by over two centimeters, at which point samples were collected every minute for up to 24 minutes. Like the precipitation containers, the collection containers for the ISCO samples were lined with mineral oil to minimize isotopic evaporative enrichment between sample collection in the autosampler and the following morning, when samples were transferred to 4ml vials and stored in the dark as described for precipitation samples. The samples collected from the ARS sediment sampler did not use mineral oil, but were otherwise treated identically. All runoff samples were collected at the exit of the flume (Figure 6, red). Unfortunately, over the summer of 2015 monsoon season, only one runoff event was large enough to trigger sample collection, which occurred on 7/30/2015.

Lab Methods

Liquid Samples

Liquid samples (rainfall, runoff, soil water from lysimeters) were filtered and measured for Deuterium and Oxygen-18 (δD and δ^{18}O) on a Finnigan Delta S gas-source isotope ratio mass spectrometer (IRMS). δD was determined by Cr reduction at 750°C, coupled to the mass spectrometer; δ^{18}O was determined by CO_2 equilibrium at 15°C, coupled to the mass spectrometer. Standardization is based on internal reference materials VSMOW (precision $<\pm 0.9$ ‰ δD, $<\pm 0.08$ ‰ δ^{18}O). Precision is based on the repetition of internal standards. Each sample was run six times before moving to the next sample. Internal standard checks were inserted into the sample sequence after every sample for quality control.

Select samples were also analyzed for F, Cl, Br, NO_3 and SO_4 concentrations on a Dionex Ion Chromatograph (IC) model ICS-3000 using an AS17 analytical column (precision $<\pm 2\%$). In order to address the primary question of runoff source composition, the samples chosen to be analyzed include: all of the runoff samples collected from the ISCO autosampler and sediment sampler (n = 17 and 4, respectively); all soil water samples that had sufficient sample volume after mass spectrometry analysis, from 7/26/2015 to 8/6/2015 (the start of sample production to one week after the 7/30/2015 runoff event) (n = 26); and precipitation samples from 7/16/2015 (two weeks before the 7/30/2015 runoff event) to 7/30/2015 (n = 37). Standard checks occurred after every fifth sample.

Soil Samples

Soil samples were analyzed at the University of Arkansas Stable Isotope Lab using a continuous flow technique, where a Thermal Conversion Elemental Analyzer (TC/EA)

interfaced to a Delta Plus XP isotope ratio mass spectrometer (Gehre and Strauch, 2003). The soil samples were prepared in silver capsules (~0.3 mg) and pyrolyzed at 1425°C to convert Oxygen to CO and H_2 gas and allow them to be separated by a 1m 5A Mol sieve gas chromatography column. Raw δD and δ^{18}O values were obtained through comparison to a monitoring gas, CO or H_2. Data normalization was achieved using known standards to place values on international scales.

Unfortunately, the results of the soil sample analysis were inconclusive because results show very large daily variability (up to almost 12 ‰ δ^{18}O and 6 ‰ δD). It was therefore assumed that the soil samples were contaminated by environmental conditions and improper collection techniques, and that soil sample analysis should not be further examined when determining the results of this study. These data are available in Appendix C.

Modeling

The Kinematic Erosion and Runoff Model (KINEROS2) watershed model (Goodrich et al., 2012) was used to estimate the relative contributions of different parts of the Lucky Hills watershed 103 to the runoff in the streambed. Geometric, hydraulic, infiltrative and erosive characteristics, as well as initial model parameters are derived by intersecting KINEROS2 overland flow modeling elements with topography (lidar, ~1 x 1 m), soils, and land cover data using the Automated Geospatial Watershed Assessment (AGWA) tool (Miller et al., 2007). KINEROS2 is an event based model that requires pre-rainfall-runoff event initial soil moisture. Therefore, soil moisture sensors installed in the Lucky Hills watershed complex were used to determine the soil moisture conditions antecedent to the runoff event at LH-103 on 7/30/2015 in order to model the outflow, peak flow and total infiltration of the event. In the KINEROS2

model, the LH-103 watershed was subdivided into 18 overland flow modeling elements (polygons depicted in Figure 8, Table 1), which flowed into channel modeling elements ending at the LH-103 runoff measuring flume and slot sediment sampler. The modeled outflow data, in combination with Thiessen polygons, was used in determining the importance of the samples at each rain gauge in the overall analysis. The outflow from each of the 18 elements was assigned to the Thiessen polygon they each respectively fell under, and the ratio of the outflow from each Thiessen polygon to the total outflow was used to weigh the precipitation data when comparing the rainfall to the runoff (Table 2).

Data Archiving

The precipitation, soil water and runoff samples that were analyzed following the 2015 monsoon can be accessed in Appendices A and B. Appendix A features the isotope datasets, while Appendix B features the solute chemistry datasets. The dataset for the soil samples that were analyzed, but chosen not to be used in this research, are presented in Appendix C.

3. RESULTS

Isotopic Analysis

Mineral oil was determined to be an essential asset in reducing evaporative enrichment. Figures 9 and 10 show sample pairs from the same location and storm, where one sample is from a collector using mineral oil and the other is from an adjacent collector without mineral oil. Here, the orange line represents a 1:1 line, which the sample pairs, represented by circles, fall below. The size of the circle represents the accumulated storm depth. It is clear that without mineral oil, the samples undergo significant evaporative enrichment, especially in the case of small samples. Therefore, all samples used in the following results are samples that were collected using mineral oil.

Precipitation samples were used to determine the local meteoric water line (LMWL) of the 2015 monsoon season at both the Lucky Hills [Eq. 1] and Kendall [Eq. 2] subwatersheds.

$$\delta^2 H_{Lucky\ Hills} = 6.264 * \delta^{18}O - 3.1064 \quad \text{[Eq. 1]}$$

$$\delta^2 H_{Kendall} = 4.711 * \delta^{18}O - 12.927 \quad \text{[Eq. 2]}$$

The Lucky Hills LMWL in the present study is similar to the LMWL for the entire WGEW found by Koch (2005) [Eq. 3], as well as the long-term summer LMWL for the Tucson Basin found by Eastoe and Dettman (2016) [Eq. 4]:

$$\delta^2 H_{Walnut\ Gulch} = 6.12 * \delta^{18}O - 0.99 \quad \text{[Eq. 3]}$$

$$\delta^2 H_{Tucson\ Basin} = 6.30 * \delta^{18}O - 4.51 \quad \text{[Eq. 4]}$$

The LMWL of both subwatersheds fall below, and are significantly different from the global meteoric water line (GMWL) equation [Eq. 5] (Clark and Fritz, 1997), according to an analysis of covariance (ANCOVA) test (Figure 11).

$$\delta^2 H_{GMWL} = 8.13 * \delta^{18}O + 10.8 \quad \text{[Eq. 5]}$$

Precipitation isotope values varied temporally and spatially within and across the subwatersheds (Figures 12 - 15). At Lucky Hills, the average standard deviation across the five collecting locations was found to be 1.98 ‰ for δD and 0.65 ‰ for δ^{18}O (n = 5). At Kendall, the average variability across the four collecting locations was found to be 1.35 ‰ for δD and 0.62 ‰ for δ^{18}O (n = 2). The sampling variability, determined by the average standard deviation of adjacent collectors, was found to be 0.93 ‰ for δD and 0.43 ‰ for δ^{18}O (n = 14). Adjacent collectors at Kendall were not analyzed, so the sampling variability is unknown to this study. At Lucky Hills, where more precipitation samples were analyzed, the spatial variability decreased with increasing accumulated precipitation (Figure 16).

The soil water collected by the lysimeters at Lucky Hills and shown in Figures 17 and 18 shows trends that may be of interest to future studies. Recall that the soil at the Kendall subwatershed never became moist enough to produce lysimeter samples, so all results and discussion regarding soil water will focus on samples from the Lucky Hills subwatershed. The first lysimeter sample became available at the furthest lystimeter from the flume at the most shallow depth (LY-21m40cm) on 7/26/2015, two days after the previous storm event on 7/24/2015 and four days before the runoff event on 7/30/2015. Prior to the rains on 7/23 and 7/24/2015, there were only small storms (<0.5 cm) at the site with one exception on 7/08/2015 (0.6 cm). According to a student's t-test, the lysimeter water leading up to the rain on 7/30/2015 is not significantly different than the weighted precipitation data from 7/30/2015 ($p > 0.05$ for δ^{18}O and δD). The standard deviation assigned to the precipitation during the t-test was the sampling variability for precipitation (0.93 ‰ for δD and 0.43 ‰ for δ^{18}O).

The 60cm depth lysimeter water, which became available only after the runoff event (due to sufficient soil moisture), is more depleted in both D and ^{18}O than any of the recorded

precipitation (on 7/31/2015, δ^{18}O value of -10 ‰ and -9 ‰ for LY-9m60cm and LY-21m60cm, respectively; δD value of -77 ‰ and -70 ‰ for LY-9m60cm and LY-21m60cm, respectively). While the isotope values from the 40cm depth lysimeters remained relatively stable, the 60cm depth lysimeter water became enriched in ^{18}O and D with time.

The 2015 monsoon season was unusually dry, and only produced one significant runoff event, which occurred at the Lucky Hills subwatershed on 7/30/2015 corresponding to a storm of approximately 1.27 cm (0.5 inches). Figures 19 and 20 depict a time series of the runoff after the runoff was significant enough to trigger collection by the ISCO sampler. In Figure 19, the runoff becomes isotopically depleted in ^{18}O and D with time, while the δ^{18}O variability shown in Figure 20 looks to be within normal machine and sample variability ranges.

To determine the source water of the runoff, all three water sources (precipitation, soil water and runoff) can also be plotted in a 2-D plot of δD vs. δ^{18}O (Figure 21). The runoff, weighted by the change in accumulated runoff (Table 3), plots to the left and down from both the rainfall and soil water samples leading up to the runoff event, indicating that the weighted runoff is more depleted in both water isotopes than the two potential source waters (precipitation and soil water). A Student's t-test analysis comparing the weighted precipitation and weighted runoff data indicates that the precipitation and runoff are statistically different ($p < 0.05$ for both δD and δ^{18}O). A similar student's t-test was performed to compare the soil water data leading up to the runoff event (in the period from 7/26/2015 – 7/30/2015) and the weighted runoff, which showed that runoff is statistically different from the soil water when comparing δ^{18}O ($p < 0.05$), but not when comparing δD ($p > 0.05$). Because this research directly addresses the WGEW precipitation and runoff isotope data observed by Koch (2005), in Figure 22 we replicate his Figure 4.11, and add the runoff and precipitation data from the 2015 monsoon.

Solute chemistry

The sources of runoff water can also be evaluated using major ion chemistry, in combination with stable water isotopes, in precipitation, soil water, and runoff. In Figure 23, the chemistry values from the 7/30/2015 runoff event plot tightly on a 1:1 line with the other rainfall events from 7/18/2015 to 7/30/2015 at Lucky Hills, while the soil water plots with much higher concentrations of both SO_4 and Cl. Figure 24 also shows the runoff water grouping tightly with the precipitation data with respect to the SO_4/Cl ratio. The soil water consistently plots with larger SO_4/Cl values than the precipitation and runoff.

4. DISCUSSION

At the semi-arid WGEW, following observations by Goodrich et al. (2004), runoff water from ephemeral streams has been assumed to be isotopically indistinguishable from precipitation water (Baille et al. 2007). However, data from Koch's master's thesis (2005) suggests the significant presence of soil water in runoff samples at the Kendall subwatershed of the WGEW. The disparity between Koch and the observations and assumptions by Goodrich et al. and Baillie et al., respectively, inspired the present study in determining the water sources contributing to runoff. The lack of a runoff event(s) at Kendall for the 2015 monsoon season made it impossible to analyze runoff composition at that subwatershed. Even though a single runoff event was available at Lucky Hills, the statistical and graphical comparison of geochemical tracers found in precipitation, soil water, and runoff prior to, and from that event indicate that the runoff water on 7/30/2015 was likely entirely consistent with precipitation, but that more research is necessary to confirm our observations. We will discuss our conclusion by first interpreting the solute tracer results, and then the isotope tracer results. We will also mention the trends we observed in the precipitation and soil water data, which are secondary to our research but may be of interest to future studies, and finally we will discuss uncertainties associated with our collection techniques and the data we selected to draw our conclusions.

Source of runoff

Using graphical interpretations of the solute chemistry of precipitation, soil water and runoff on and surrounding the 7/30/2015 runoff event, we can infer that soil water is not present in the runoff, or is only present in negligible amounts. Since dissolved SO_4 and Cl are affected simultaneously by evaporation, samples that plot on a 1:1 line when plotted for [SO_4] vs. [Cl]

(Figure 23), or on a horizontal line when plotted for $[SO_4]/[Cl]$ vs. $\delta^{18}O$ (Figure 24), might be interpreted as samples from the same source, undergoing varying amounts of evaporation. Our results therefore show that soil water and precipitation are unique, since the soil water plots far above the 1:1 line of precipitation and with much larger $[SO_4]$ to [Cl] ratios (likely due to longer exposure time to soil minerals). Precipitation and runoff water samples from 7/30/2015 (the day of the single runoff event of 2015) plot together on the 1:1 line and have similar values of both $[SO_4]$ and [Cl], suggesting runoff at Lucky Hills is entirely composed of precipitation water, with no or negligible mixing with the soil water. As shown by Figures 23 and 24, the results of ion chromatography analysis suggest that precipitation is the only significant source in the runoff water at Lucky Hills.

Despite the conclusive findings of the solute chemistry graphs, statistical hypothesis tests comparing the stable isotope values of water (^{2}H and ^{18}O) in the three sources (precipitation, soil water and runoff) reveal that precipitation and runoff are, in fact distinct. The weighted precipitation is more enriched in both ^{2}H and ^{18}O than the weighted runoff, so the distinct isotope values cannot be explained by isotopic evaporative enrichment of the runoff water in-stream and before collection. However, it is possible that the precipitation collected before and after the production of runoff are influencing the isotope composition of the daily composite sample to look more enriched than that of runoff. The results of the isotope analysis do not contribute a clear understanding of the source composition of the runoff; therefore, we choose to base our conclusions largely off of the solute chemistry analysis.

While Koch (2005) found evidence that soil water may be mixing into the runoff at the Kendall subwatershed of the WGEW, it is important to note that at the Lucky Hills subwatershed, he found rainfall and runoff to have similar isotope values (Figure 22). Goodrich

et al. (2004) also found precipitation and runoff to have similar δ^{18}O and δD values at the main channel in Walnut Gulch (a larger spatial scale), which is what led Baillie et al. (2007) to make the assumption that precipitation and runoff data samples are isotopically interchangeable. Therefore, the results of this research are consistent with previous studies at Lucky Hills, but more research is needed in order to determine if the results observed in this paper are valid for all parts of the WGEW.

Secondary Results

The shallow slopes of the Lucky Hills and Kendall local meteoric water lines (LMWLs) compared to the Global Meteoric Water Line (GMWL) (Figure 11) indicate that evaporation occurs during precipitation. This trend is common in semiarid regions, since the lighter δD is preferentially evaporated over the heavier δ^{18}O (Gat 1980). Conditions controlling evaporation are highly variable temporally and spatially, which might explain why the composite LMWL of the WGEW observed by Koch (2005), is slightly different from the LMWLs of the Lucky Hills and Kendall subwatersheds found in this study (Figure 11). The relative contributions of the different vapor sources to the precipitation (generally, the Gulf of Mexico and Caribbean versus the Pacific Ocean and Gulf of California) will also affect the LMWL of any given year, and may explain slight variations between our data, Koch (2005) and the long-term Tucson Basin summer LMWL (Eastoe and Dettman, 2016) (Figure 11).

Storm size is seen to affect the spatial variability of the samples collected at Lucky Hills (Figure 16). According to the "amount effect" originally studied by Dansgaard (1964), small storms are more subject to isotopic evaporative enrichment than large storms, since small raindrops equilibrate to a larger degree with the water vapor and temperature conditions below

the cloud base, and they evaporate relatively more than larger raindrops on their way to the land surface. Large raindrops, on the other hand, retain their δD and δ^{18}O values due to longer equilibration times and larger volume (Dansgaard, 1964). Since the amount of evaporative enrichment small raindrops experience is determined by temperature and water vapor conditions, which are highly variable in arid and semi-arid environments, the amount effect might explain the high spatial variability observed in precipitation during small storms at Lucky Hills (Figure 16).

Isotope time series of the soil water (Figures 17, 18) show trends that are not well studied in this paper but may be of interest to future studies. The first soil water samples became available at the shallow (40cm) depth, furthest from the flume (21.3 meters) on 7/26/2015, two days after the previous rain event (7/24/2015) and four days prior to the first and only runoff event at Lucky Hills (7/30/2015). Soil water from the other three lysimeters (21.3 meters from the flume, 60cm deep; 9.1 meters from the flume, 40cm deep; 9.1 meters from the flume, 60cm deep) became available only after the runoff event on 7/30/2015. Given that soil water samples became available before any significant runoff events, the delay between precipitation on 7/24/2015 and soil water sample generation on 7/26/2015 might suggest subsurface flow and the accumulation of soil water from upgradient sources. The samples from 60cm depths are much more depleted in ^{18}O and D than any of the other potential sources studied in this research: antecedent precipitation from the 2015 monsoon season, the recent precipitation, the 40cm soil water samples, and runoff water (Figures 21). Winter precipitation is known to be more depleted in ^{18}O and D than summer precipitation in the southwestern U.S. (Wright, 2001; Eastoe and Dettman, 2016), so it is possible that the 60-cm lysimeters are sampling water sourced from winter precipitation, or they receive flow from sources not studied in this paper. To determine if

the isotopically depleted water was in fact a result of winter precipitation, we compared the deep soil water (60 cm) to the winter-time local meteoric water lines observed by Eastoe and Dettman (2016) and Baillie et al. (2007). The local meteoric water lines did not approach the deep soil water on a 2-D δD vs. δ^{18}O plot similar to Figure 21, but because the local meteoric water lines used for comparison are not necessarily representative of the winter precipitation from 2015, the results of this comparison do not negate the possibility that the deep soil water is depleted in 18O and D as a result of winter precipitation.

The deep soil water (60 cm) also became enriched in ^{18}O and D with time (Figures 17, 18), showing either evaporative enrichment or mixing with the enriched water from above. Since the same trend is not observed in the 40cm depth samples, which would be more likely to undergo evaporation, mixing is considered to be the most likely reason for the observed increasing trend in the δD and δ^{18}O isotopes of the 60cm soil water samples.

Uncertainties

Soil Water

Suction lysimeters struggle to collect immobile water, the soil water in micropores or thin films of water tightly bound to the soil particles, at a tension above 35 centibars (Landon et al, 1999). As the water more tightly bound to the soil particle might reside in the soil for longer periods of time, it could have a different isotopic signature than the samples being extracted from the lysimeter, and the lysimeter water might not reflect the actual isotopic and signature of the soil water. However, since the tightly bound residual soil moisture would only be present at small volumes, this likely does not influence the isotope values in our soil water samples dramatically.

Dry soil moisture conditions limited our ability to collect and analyze soil water before the 7/30/2015 runoff event, since lysimeters are unable to retrieve samples below a matric water potential of 10^{-3} hPa (Sprenger et al., 2015). We were unable to pump soil water from three of the four lysimeters on 7/30/2015 prior to the runoff event, which indicates that the soil moisture conditions necessary to retrieve soil water from suction lysimeters were not present at all but one lysimeter location and depth. While lysimeter LY-21m40cm produced soil water samples before the runoff event, it would have been ideal to be able to analyze soil water from the other three lysimeters (both 60cm depth lysimeters and LY-9m40cm) as well, to get a more clear picture of the geochemical tracer concentrations in the soil water prior to the runoff event.

Limited Number of Samples Analyzed

Not all of the collected precipitation samples were analyzed. Only five out of the 24 storms collected at Lucky Hills were chosen to have samples analyzed from all of the collectors, because it was believed that five storms would be enough to establish the spatial variability in precipitation isotope signatures for individual storms. The five storms selected were chosen for a variety of reasons: all samples on 7/29/2015 and 7/30/2015 were analyzed in order to view the precipitation before and during before the runoff event on 7/30/2015; all samples on 7/31/2015 were analyzed because it was the last precipitation event before a long period of no rain, which we thought might be important when considering soil drying dynamics; and all samples on 8/9/2015 and 8/26/2015 were chosen in order to view precipitation from different parts of the monsoon season, and to consider the isotopic composition of small versus large storms. Because the spatial variability across Lucky Hills for a single storm was found to be relatively small (avg 1.98 ‰ δD, 0.65 ‰ δ^{18}O), the remaining storms used to construct the LMWL (Figure 11), and

to compare precipitation data to runoff and soil water, were analyzed for only one collector (RG-083C1). Kendall precipitation data was even less studied because it could not be applied to the main focus of this research (runoff source composition), due to the lack of runoff generation at Kendall during the 2015 monsoon season. Therefore, the LMWL at Kendall is based on all of the samples collected from only three storm events, the dates of which were chosen to coincide with the storms selected for total analysis at Lucky Hills in order to view the variability between watersheds for the same storms. This might explain the relatively low R^2 value of 0.54 for the Kendall LMWL. While in general, we believe that the choice to limit data analysis to a few select representative samples is valid for the purpose of our research, Figure 16 suggests that this may not have been the course of action for small storms, which can experience larger variability and would have been better represented by taking the average of many samples. Given that all the important dates considered in our research were either large storms or had all the samples analyzed, small storm variability is not likely to influence our conclusions about the sources contributing to the runoff on 7/30/2015. Small storm variability may, however, influence the LWML we found for Lucky Hills, and it should be considered if any of this data is used in future research.

The fact that there was only one runoff event during the 2015 monsoon season makes trend analysis a challenge for this research. All of the conclusions about runoff water composition discussed in this section are the result of only one storm, which we cannot say with confidence reflects normal conditions since there are no other runoff events from 2015.

5. CONCLUSION

We used isotope and solute geochemical tracers to determine the sources of runoff at the Lucky Hills subwatershed of the Walnut Gulch Experimental Watershed (WGEW). Graphical representations of the concentrations of chloride and sulfate in the same waters conclusively revealed that the runoff and precipitation water cannot be distinguished, while runoff and soil water are distinct. However, statistical hypothesis testing of the stable isotopes of water (^{2}H and ^{18}O) in precipitation, soil water and runoff, showed precipitation and runoff to be distinct. Therefore, it is likely that there was negligible to no soil water mixing into the runoff at Lucky Hills during the 2015 monsoon season, which is consistent with data found by Goodrich et al. (2004) and Koch (2005), and the assumptions made by Baillie et al. (2007), but additional research is necessary to confirm this conclusion. Additional research is needed to extend the conclusions of this paper beyond the Lucky Hills subwatershed of Walnut Gulch, since Koch (2005) observed trends in his research that suggest the presence of soil water in runoff at the Kendall subwatershed of Walnut Gulch.

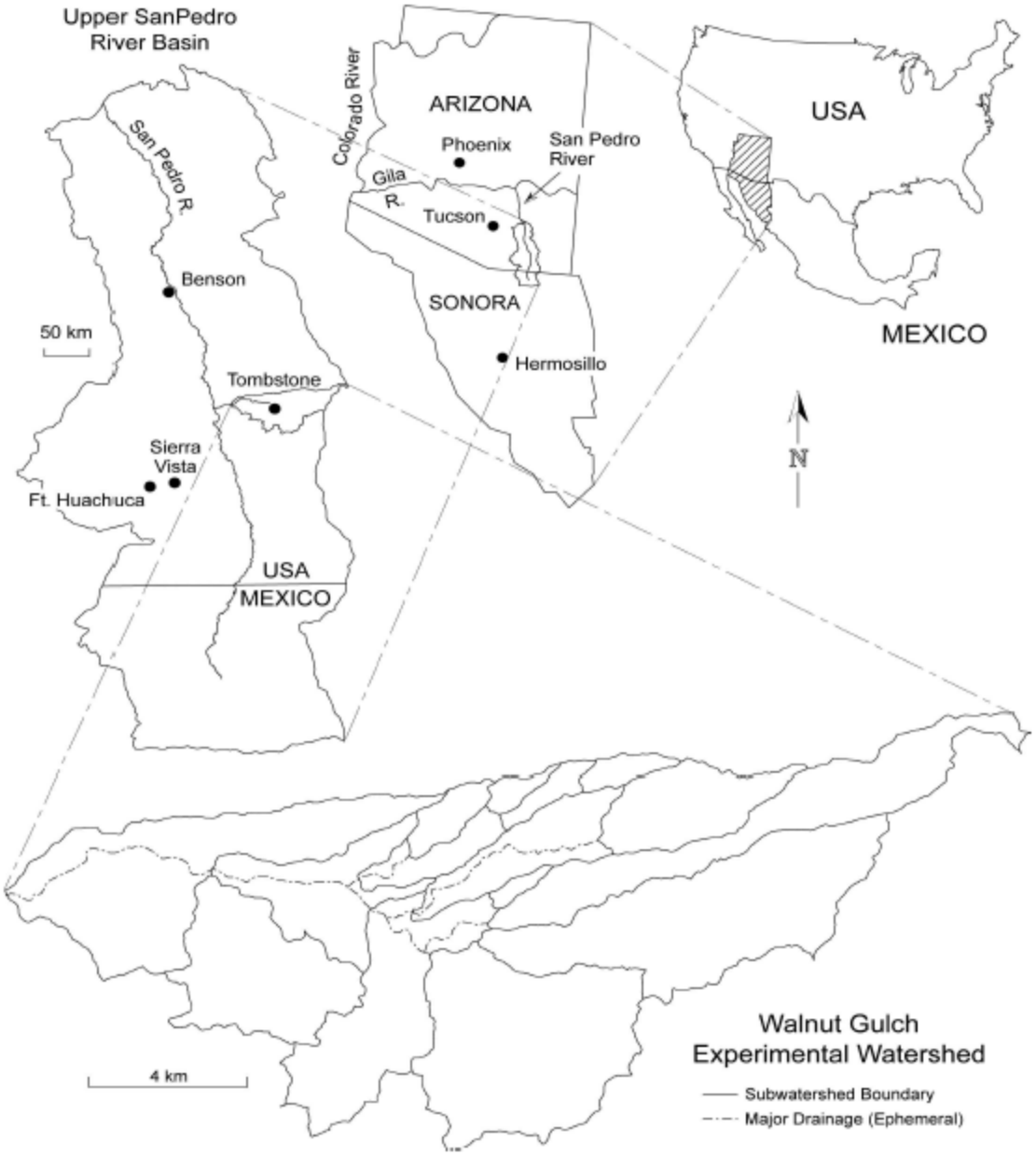

Figure 1: Map of the Walnut Gulch Experimental Watershed, showing its location in comparison to the U.S.A and Mexico; major cities and rivers in Arizona, U.S.A and Sonora, Mexico; and within the Upper San Pedro River Basin

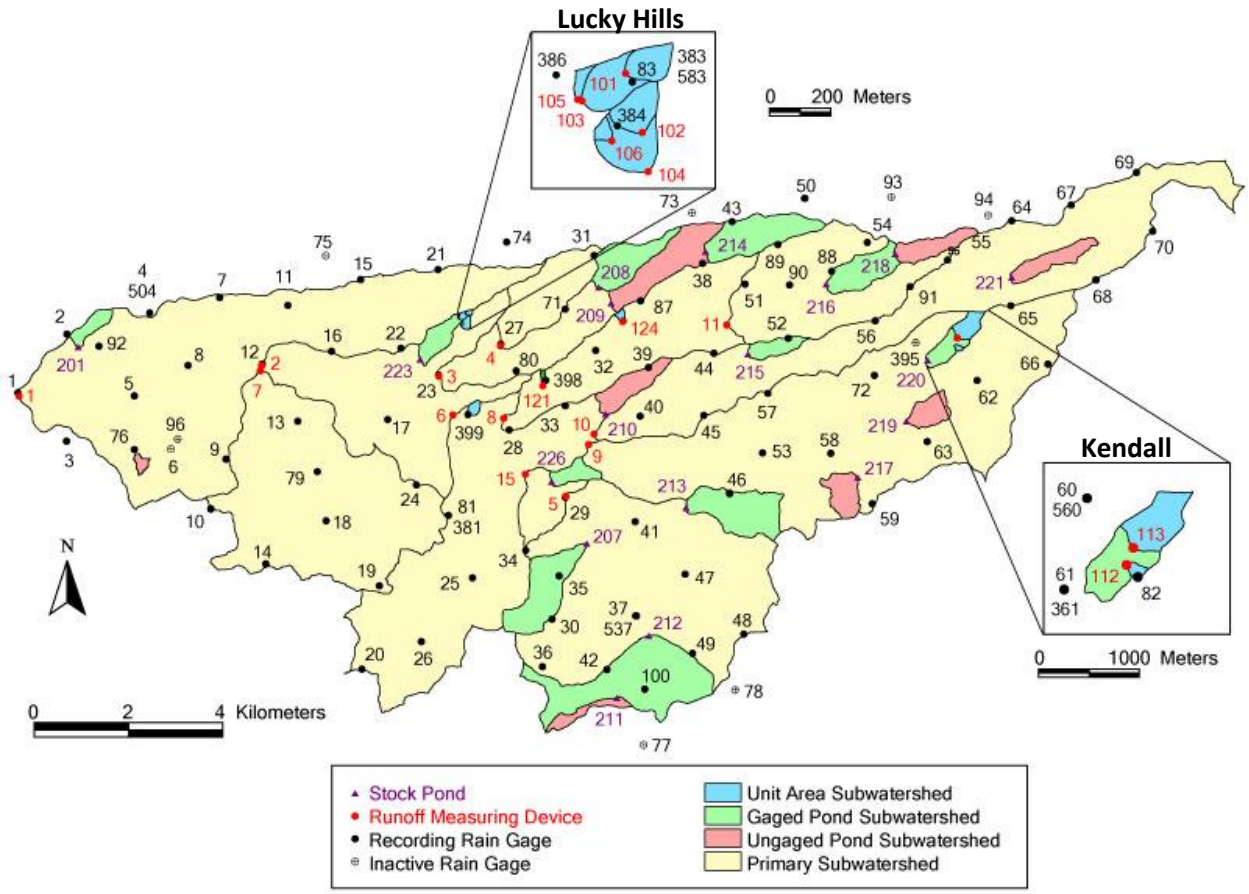

Figure 2: Locations of Lucky Hills and Kendall subwatersheds within the WGEW, and map of instrumentation at the WGEW

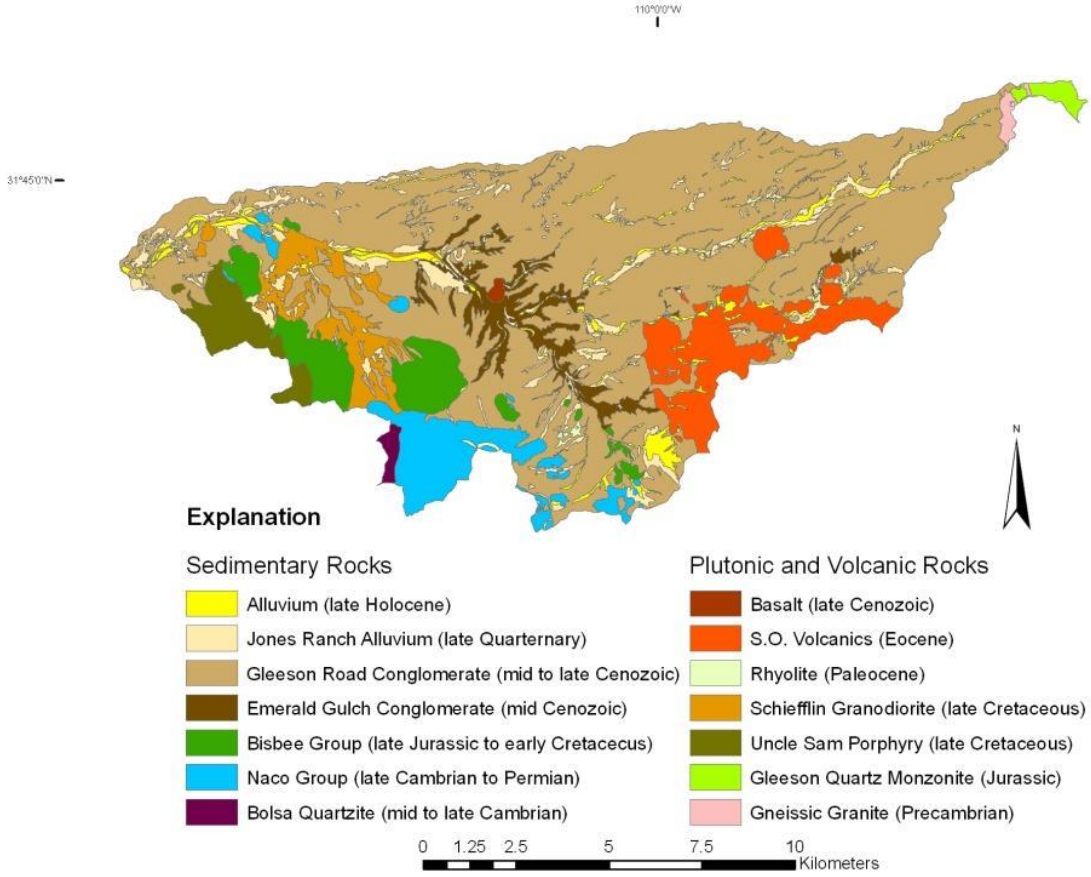

Figure 3: Geology of WGEW, showing that the WGEW is primarily Alluvium (Gleeson Road Conglomerate) from Cenezoic era

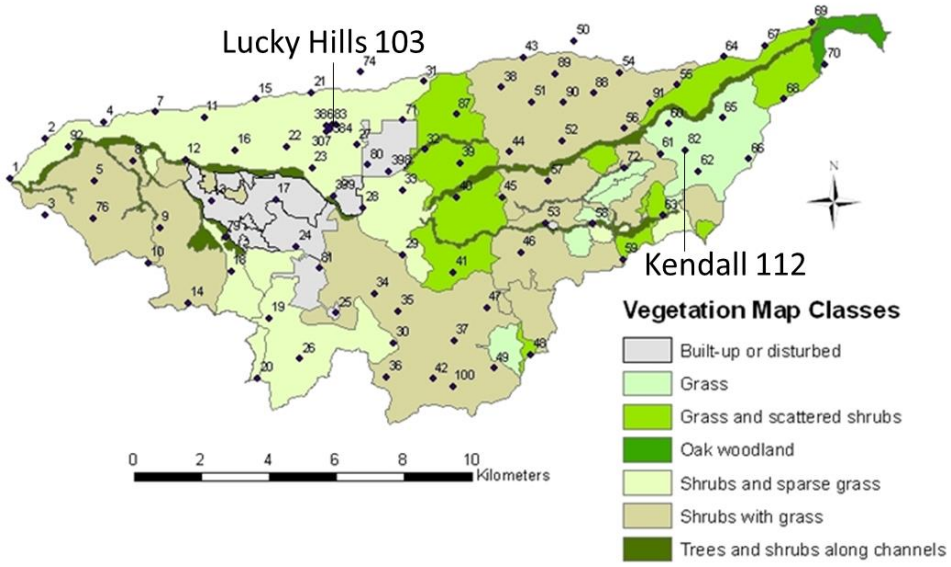

Figure 4: Vegetation survey of WGEW (Skirvin et al., 2008), with added markers to show Lucky Hills 103 and Kendall 112 subwatersheds

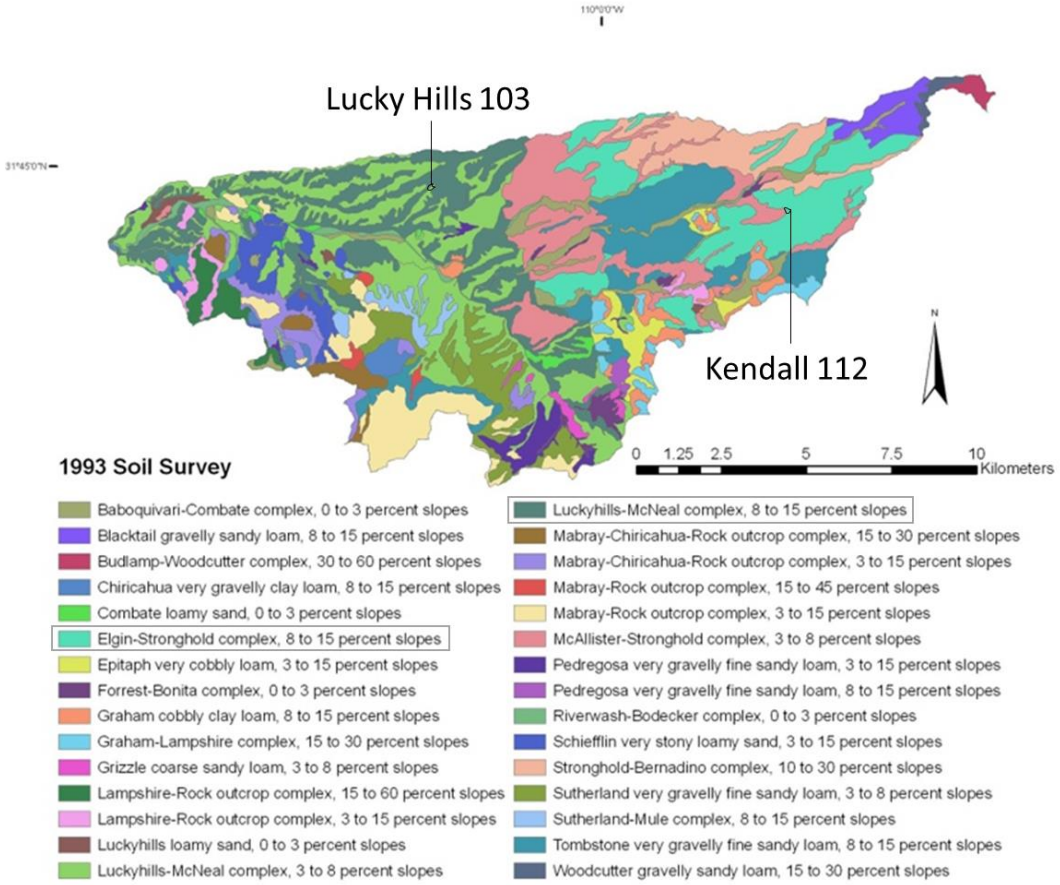

Figure 5: Soil survey of WGEW (Breckenfeld et al., 1995), with added markers to show Lucky Hills 103 and Kendall 112 subwatersheds

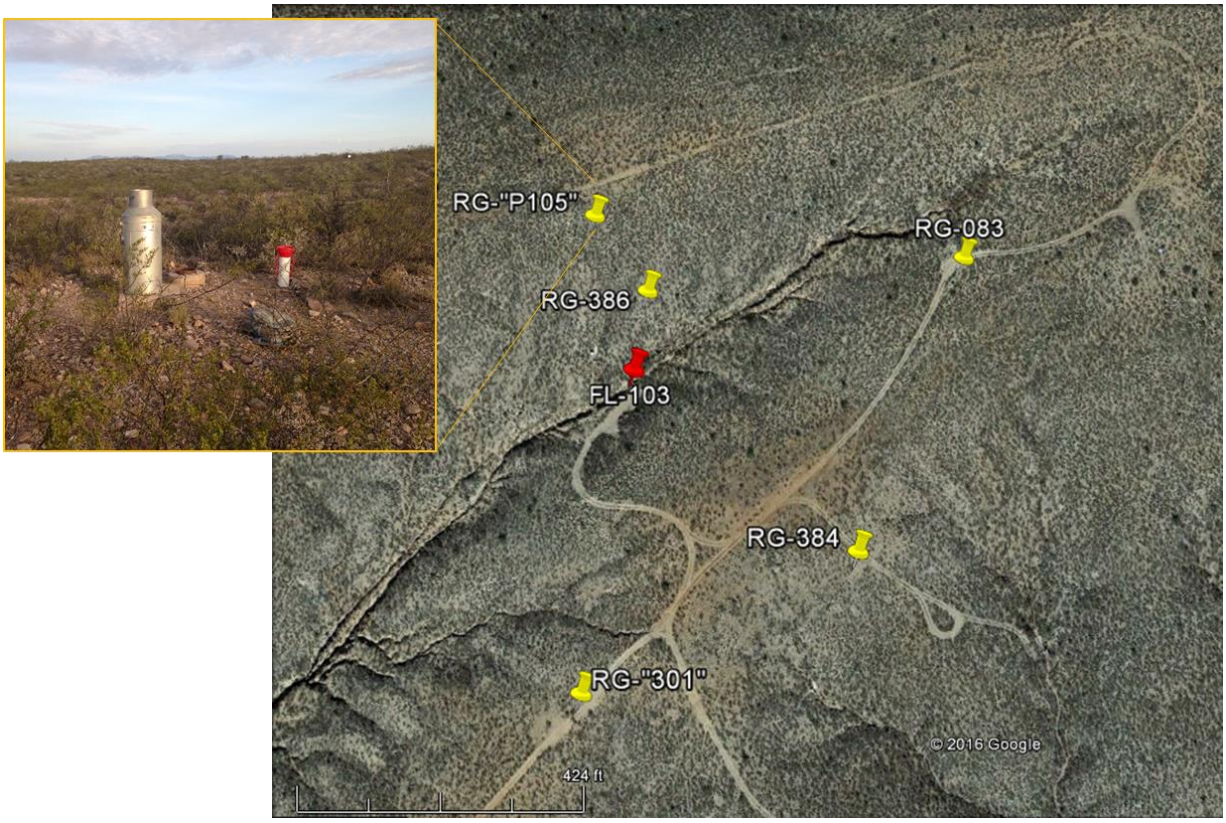

Figure 6: Aerial map of Lucky Hills watershed 103, showing precipitation collecting locations (yellow) and Flume 103 (red)

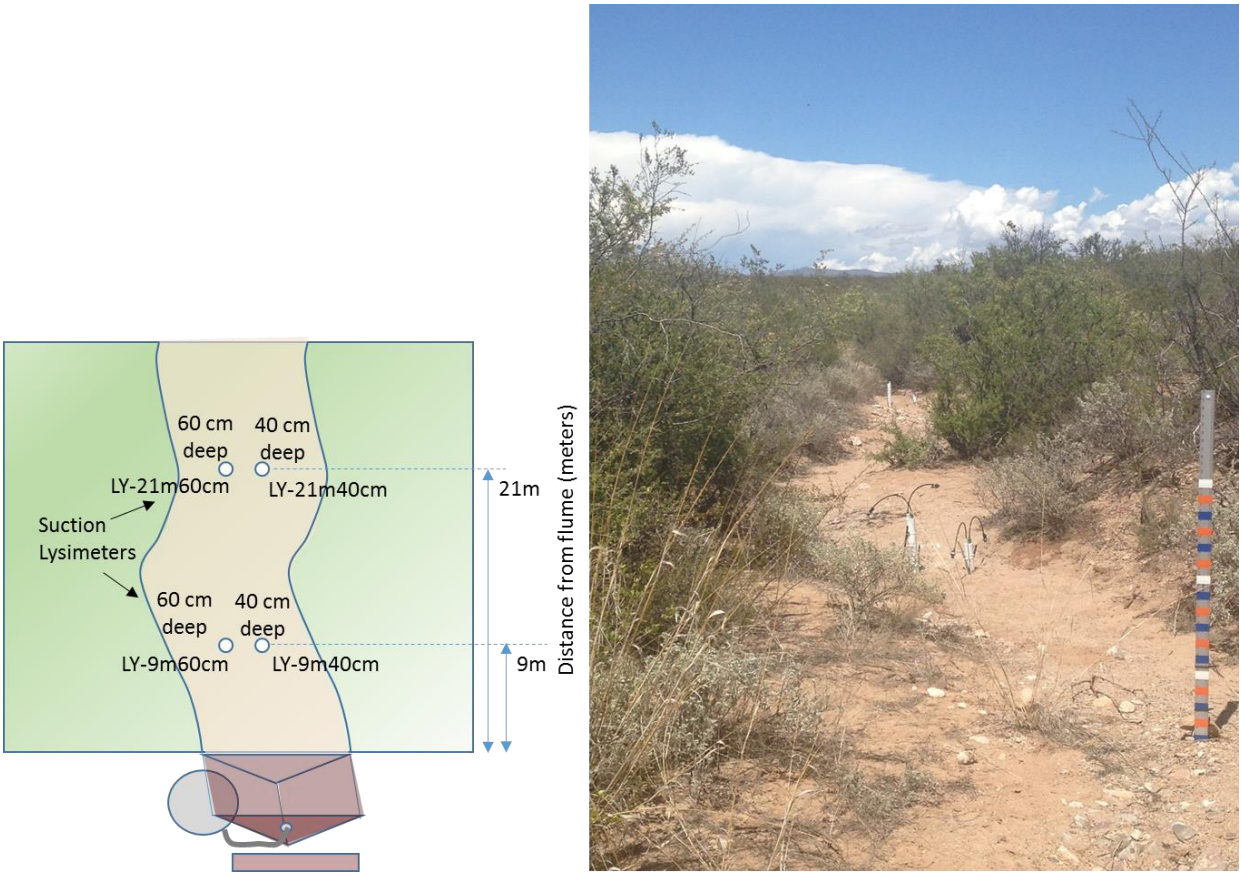

Figure 7: On the left, a graphic depiction of suction lysimeter collecting locations in the Lucky Hills 103 streambed, including their depths and distance from Flume 103; on the right, an image of the suction lysimeters in the streambed.

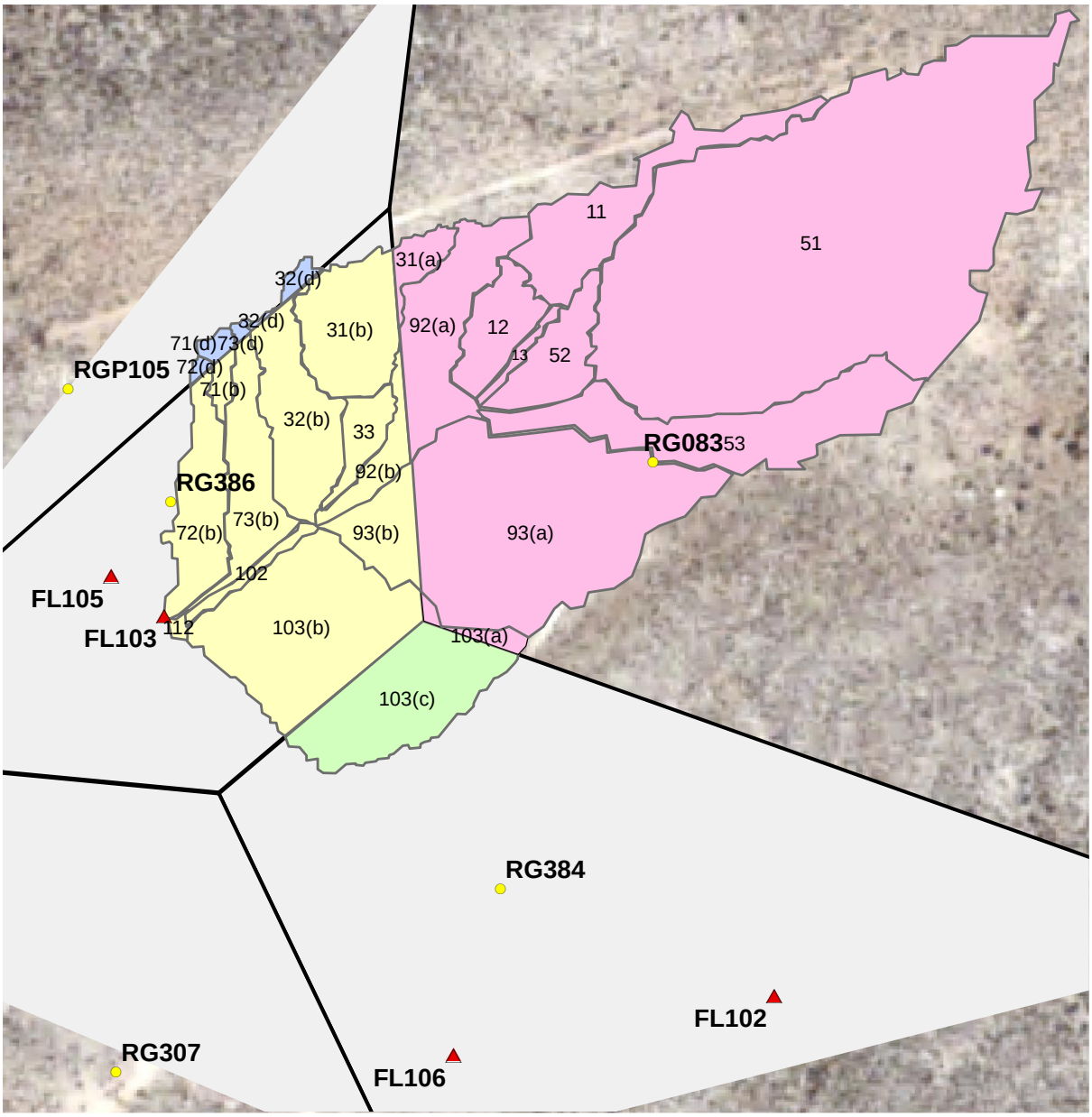

Figure 8: Map of Lucky Hills 103 catchment area, separated into small, numbered polygons by the KINEROS2 runoff modelling program, and colored according to the Thiessen polygons of each relevant rain gauge: RG-083 (pink, 'a'), RG-386 (yellow, 'b'), RG-384 (green, 'c'), RG-P105 (blue, 'd') (used in weighing precipitation on 7/30/2015)

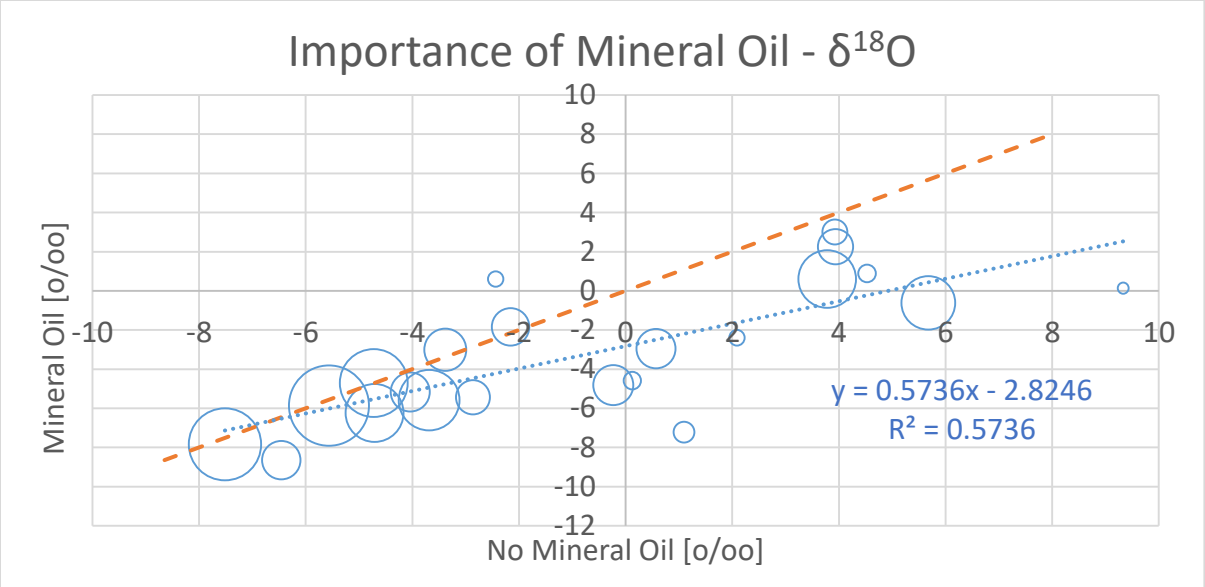

Figure 9: Importance of mineral oil in reducing $\delta^{18}O$ evaporative enrichment between precipitation event and sample collection. Circles represent adjacent data pairs from adjacent collectors with and without mineral oil. Circle size represents accumulated precipitation

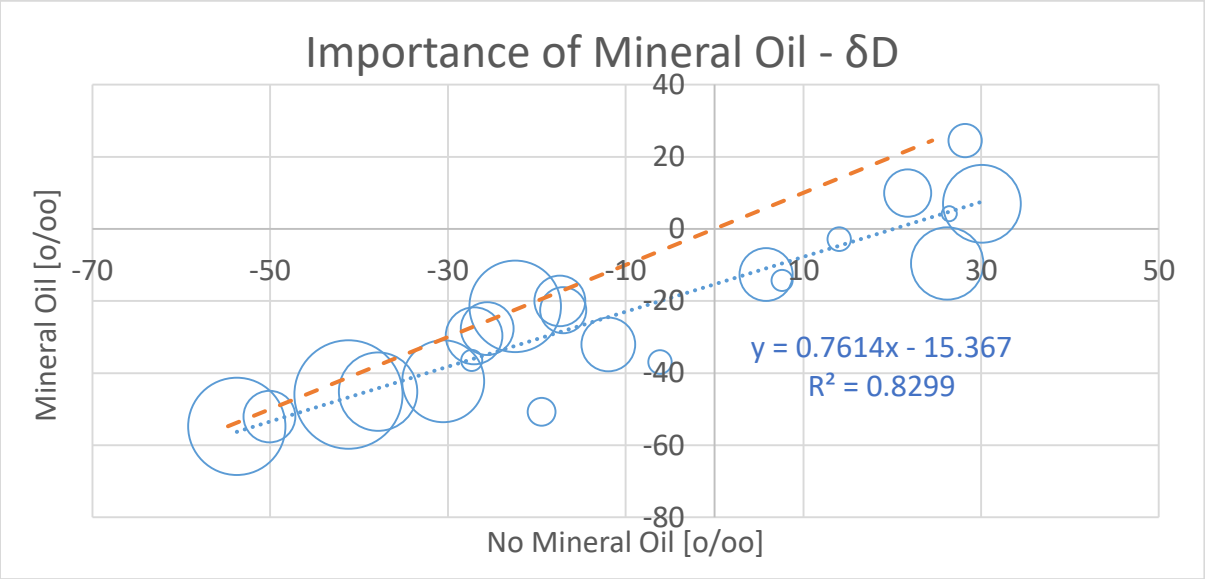

Figure 10: Importance of mineral oil in reducing δD evaporative enrichment between precipitation event and sample collection. Circles represent adjacent data pairs from adjacent collectors with and without mineral oil. Circle size represents accumulated precipitation

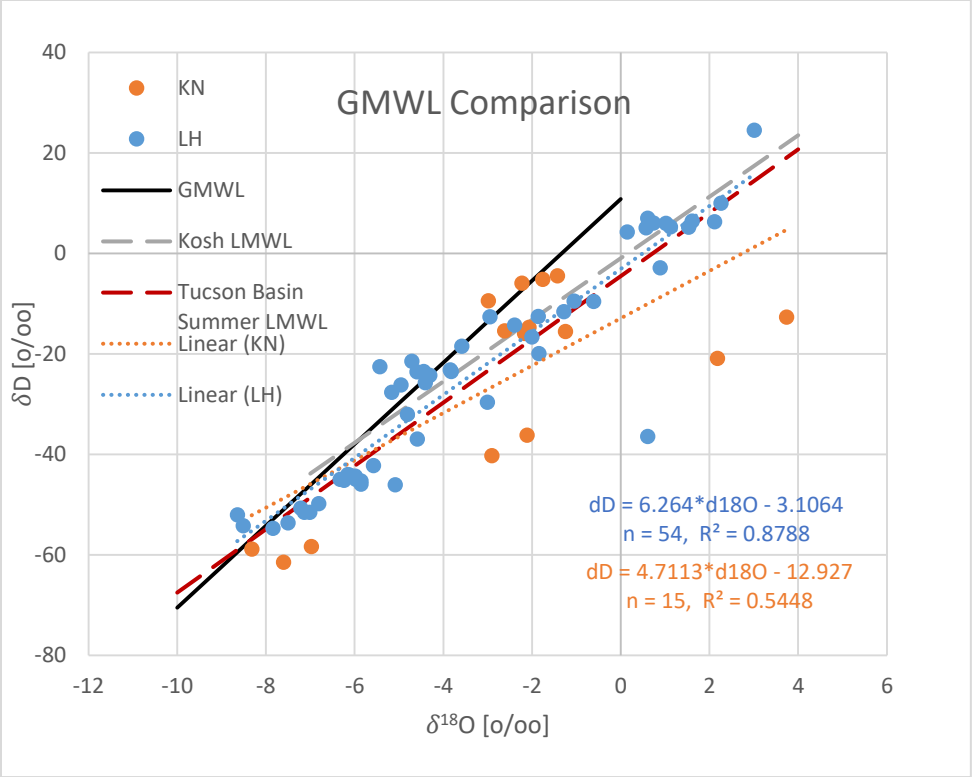

Figure 11: Precipitation values from Lucky Hills (blue) and Kendall (orange) subwatersheds, with their respective LMWLs, compared to the GMWL (black) and Koch (2005) Walnut Gulch Experimental Watershed LMWL (grey) and long-term Tucson Basin Summer LMWL (maroon) (Eastoe and Dettman, 2016)

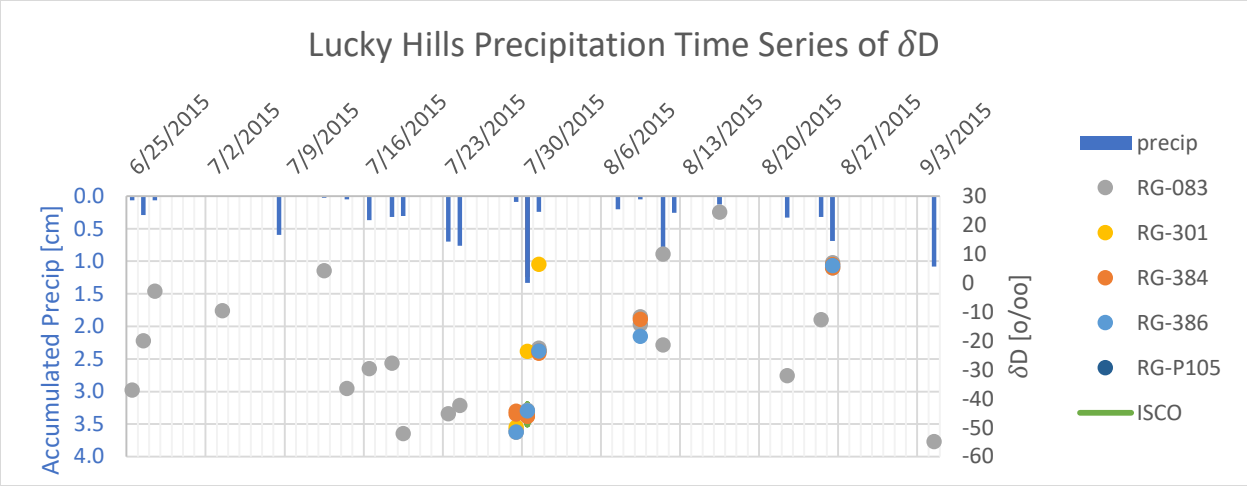

Figure 12: Time series of accumulated precipitation at the Lucky Hills subwatershed (primary vertical axis, columns); precipitation (points) and 7/30/2015 runoff (line) analyzed for δD (secondary vertical axis)

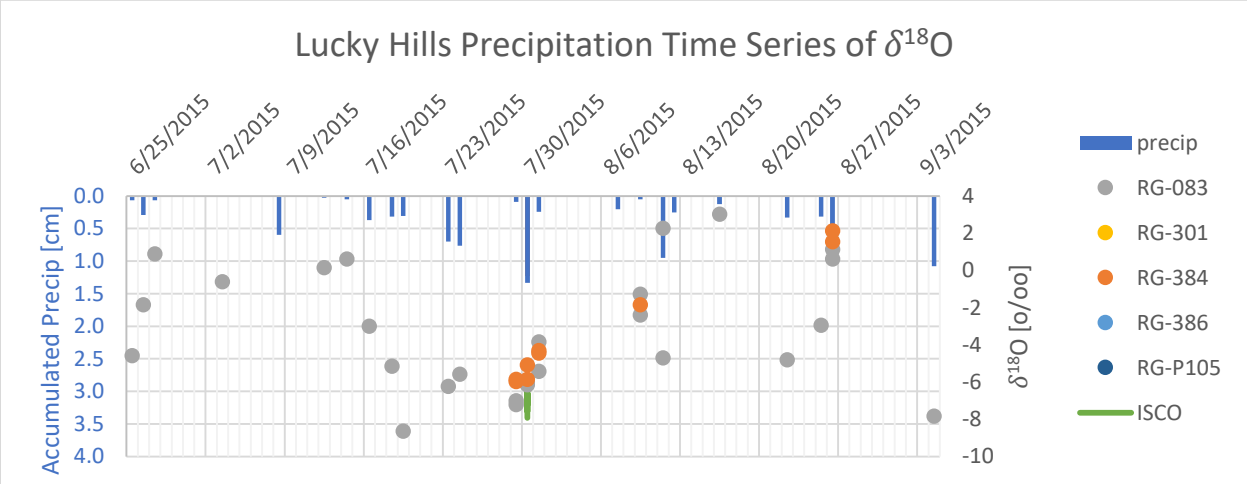

Figure 13: Time series of accumulated precipitation at the Lucky Hills subwatershed (primary vertical axis, columns); precipitation (points) and 7/30/2015 runoff (line) analyzed for $\delta^{18}O$ (secondary vertical axis)

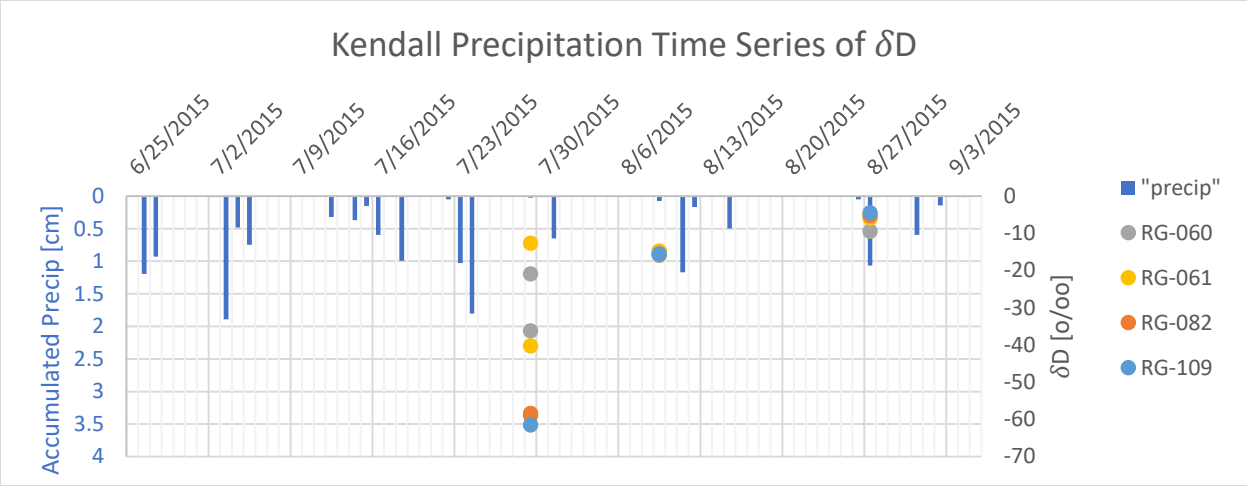

Figure 14: Time series of accumulated precipitation at the Kendall subwatershed (primary vertical axis, columns); precipitation (points) analyzed for δD (secondary vertical axis)

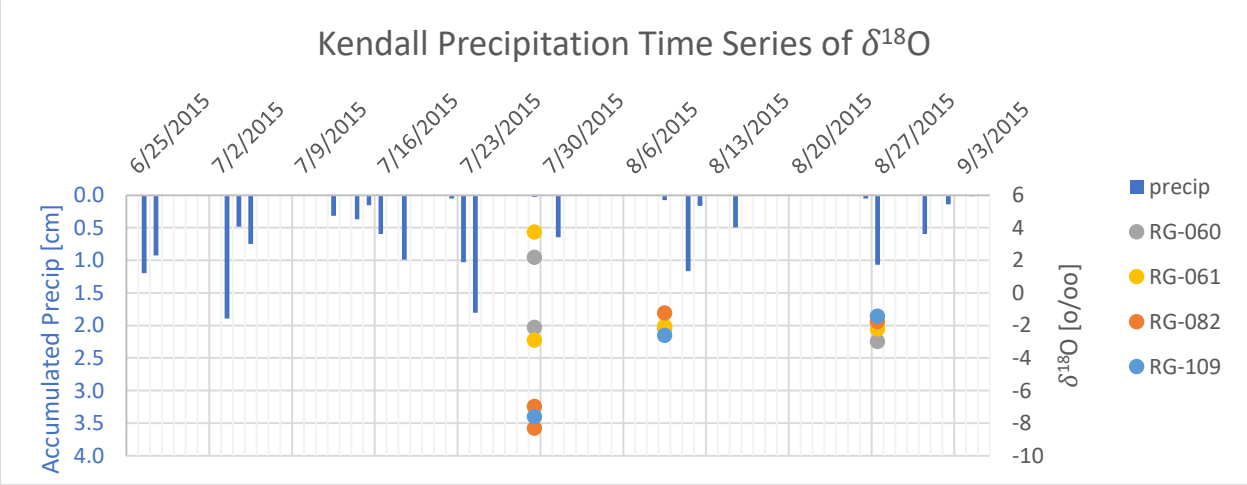

Figure 15: Time series of accumulated precipitation at the Kendall subwatershed (primary vertical axis, columns); precipitation (points) analyzed for $\delta^{18}O$ (secondary vertical axis)

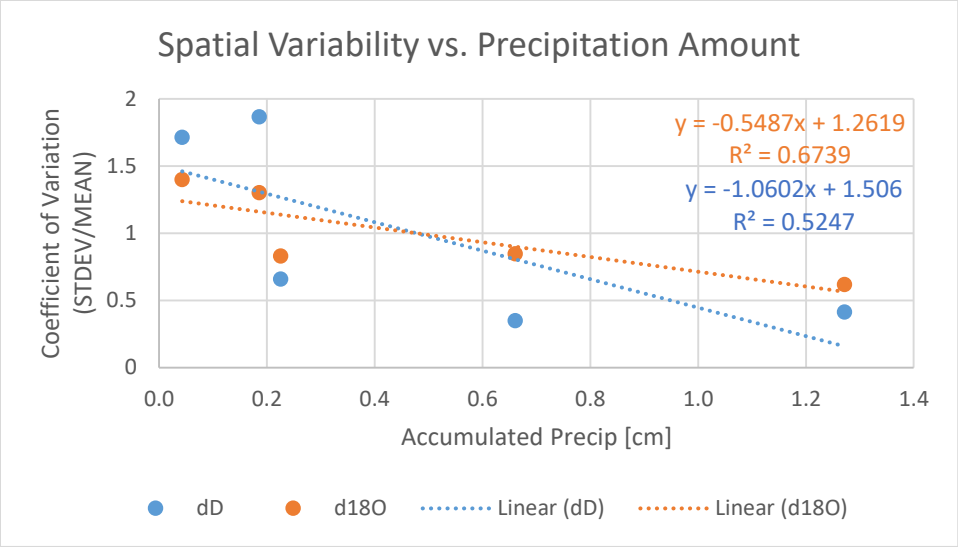

Figure 16: Decreasing variability, expressed by coefficient of variation, in δD (blue) and $\delta^{18}O$ (orange) with increasing accumulated precipitation

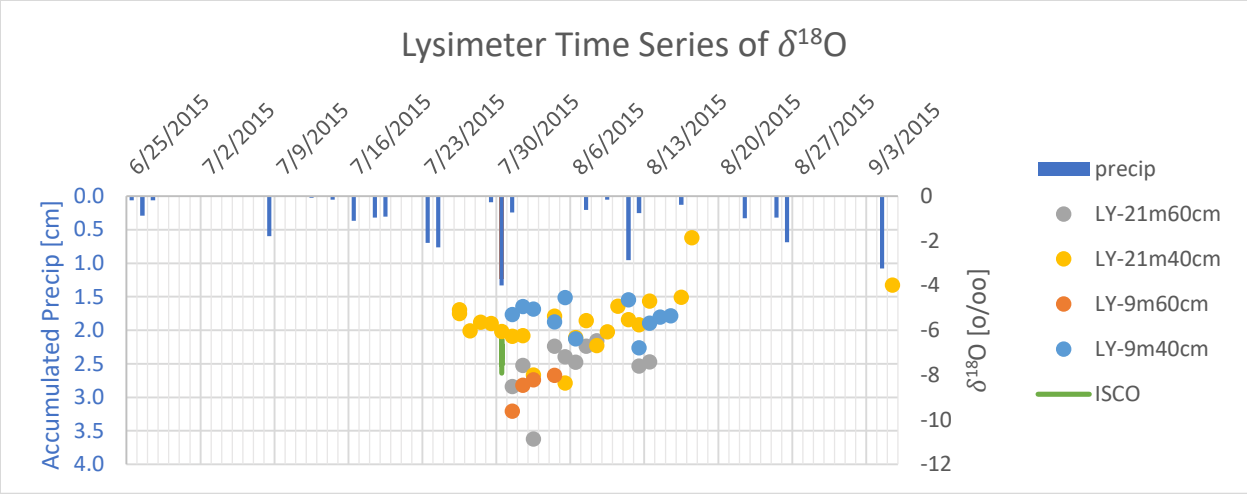

Figure 17: Time series of accumulated precipitation at the Lucky Hills subwatershed (primary vertical axis, columns); lysimeter (points) and 7/30/2015 runoff (line) analyzed for $\delta^{18}O$ (secondary vertical axis). Lysimeter samples are labeled by their distance from the flume (approximately 9 or 21 m) and depth (40cm or 60cm)

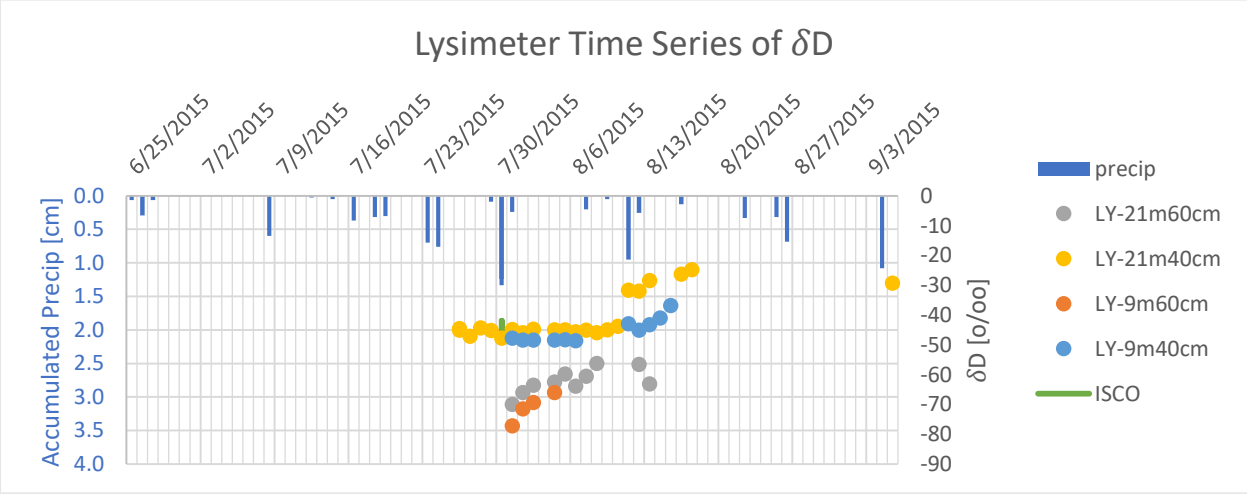

Figure 18: Time series of accumulated precipitation at the Lucky Hills subwatershed (primary vertical axis, columns); lysimeter (points) and 7/30/2015 runoff (line) analyzed for δD (secondary vertical axis). Lysimeter samples are labeled by their distance from the flume (approximately 9 or 21 m) and depth (40cm or 60cm)

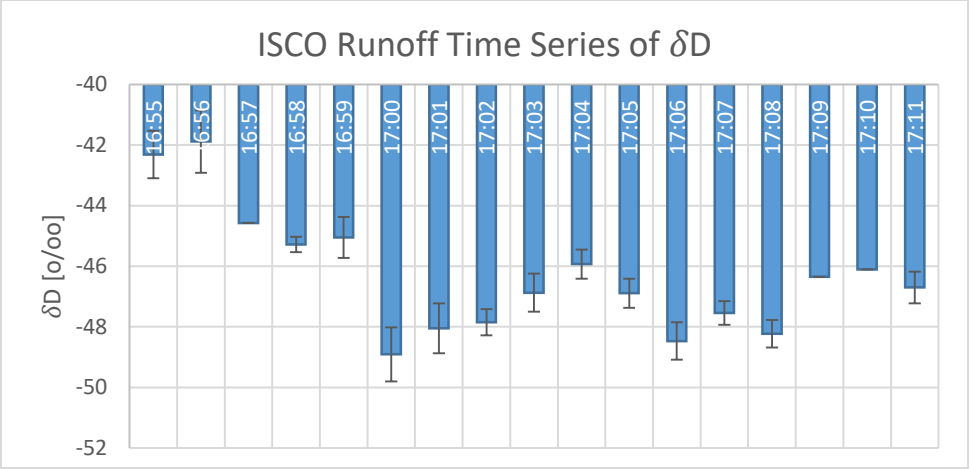

Figure 19: Time series of runoff at the Lucky Hills subwatershed on 7/30/2015, analyzed for δD. Error bars depict two times the standard deviation assigned to the data by the mass spectrometer.

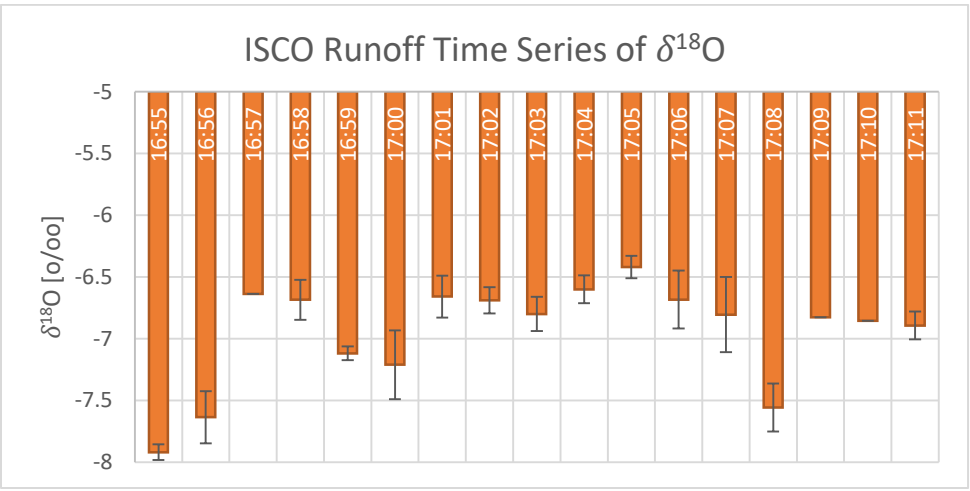

Figure 20: Time series of runoff at the Lucky Hills subwatershed on 7/30/2015, analyzed for $\delta^{18}O$. Error bars depict two times the standard deviation assigned to the data by the mass spectrometer.

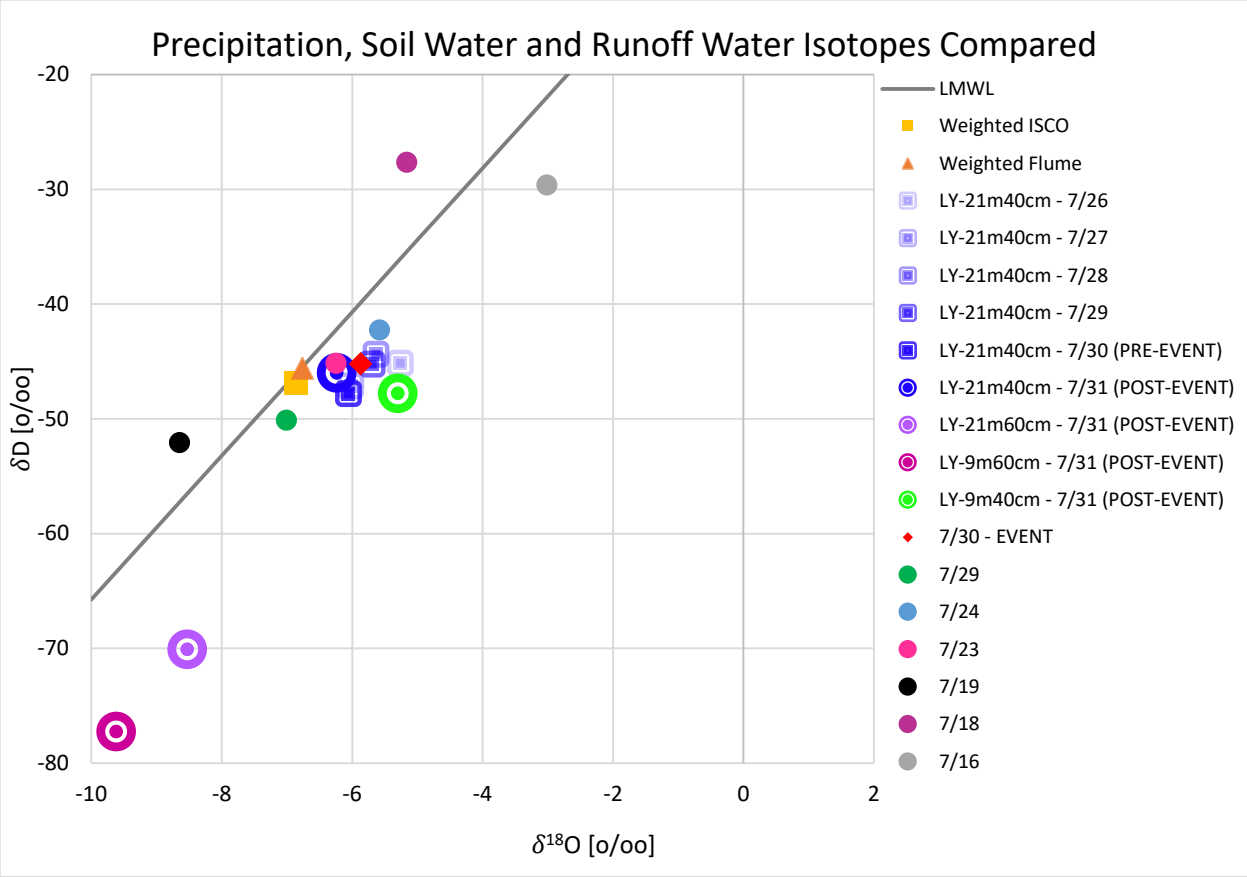

Figure 21: Isotopic comparison of the 7/30/2015 runoff event (weighted), precipitation and soil water leading up to the runoff event, and lysimeter samples the day after the runoff event. Precipitation values are unweighted averages of Lucky Hills, except the rain from 7/30/2015, which is weighted by contribution to runoff. Lysimeter samples leading up to the runoff event are depicted by square bullseyes, becoming darker with time; lysimeter samples collected the day after the runoff event are represented by circular bullseyes. Lysimeter samples are labeled by their distance from the flume (approximately 9 or 21 m) and depth (40cm or 60cm)

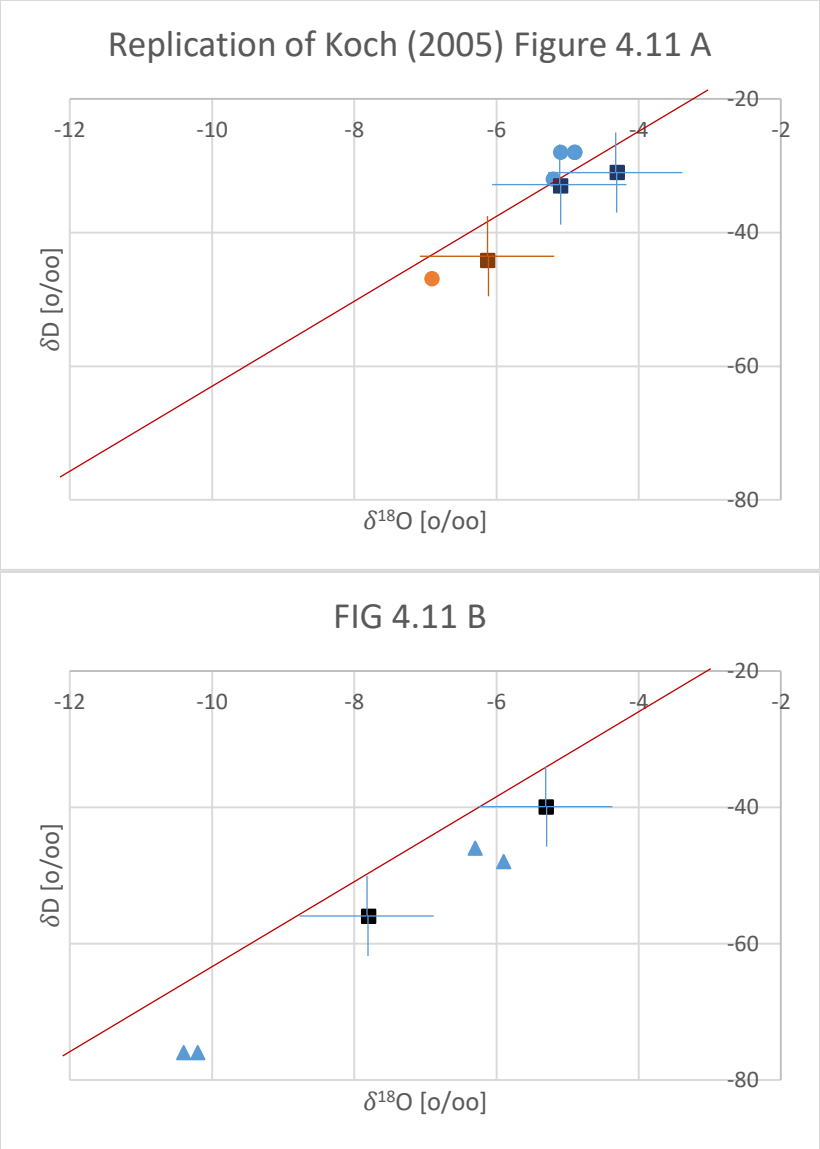

Figure 22: Replication of Koch (2005) Figure 4.11, whose data are presented in blue and navy: "$\delta^{18}O$ and δD isotopes for Lucky Hills (A) and Kendall (B). Lucky Hills flows (circles, n = 4) are similar to precipitation (squares with error bars), while [Kendall] grassland flows (triangles, n =4) fall significantly outside of [precipitation] error bars." Data from the 2015 monsoon season is added to Lucky Hills (A), presented in orange with the same error bars and LMWL (red line) used by Koch

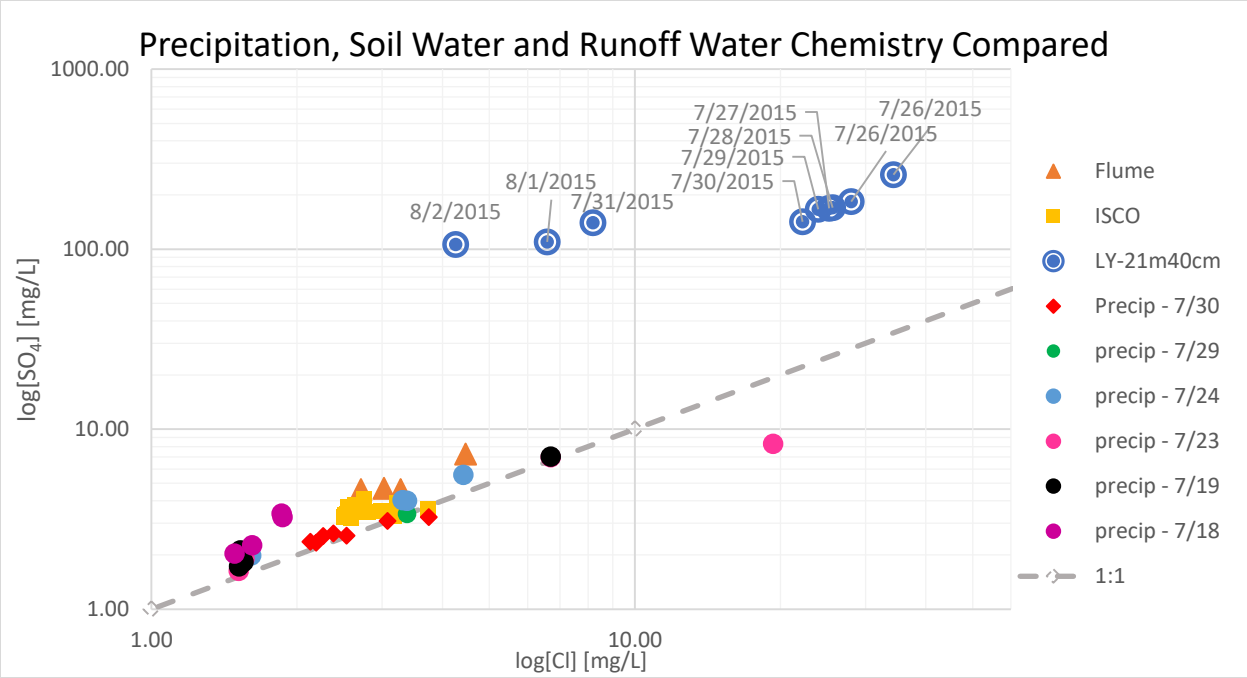

Figure 23: Comparison of precipitation (points), soil water (bullseyes), and runoff (squares and triangles) using the anions SO_4 and Cl

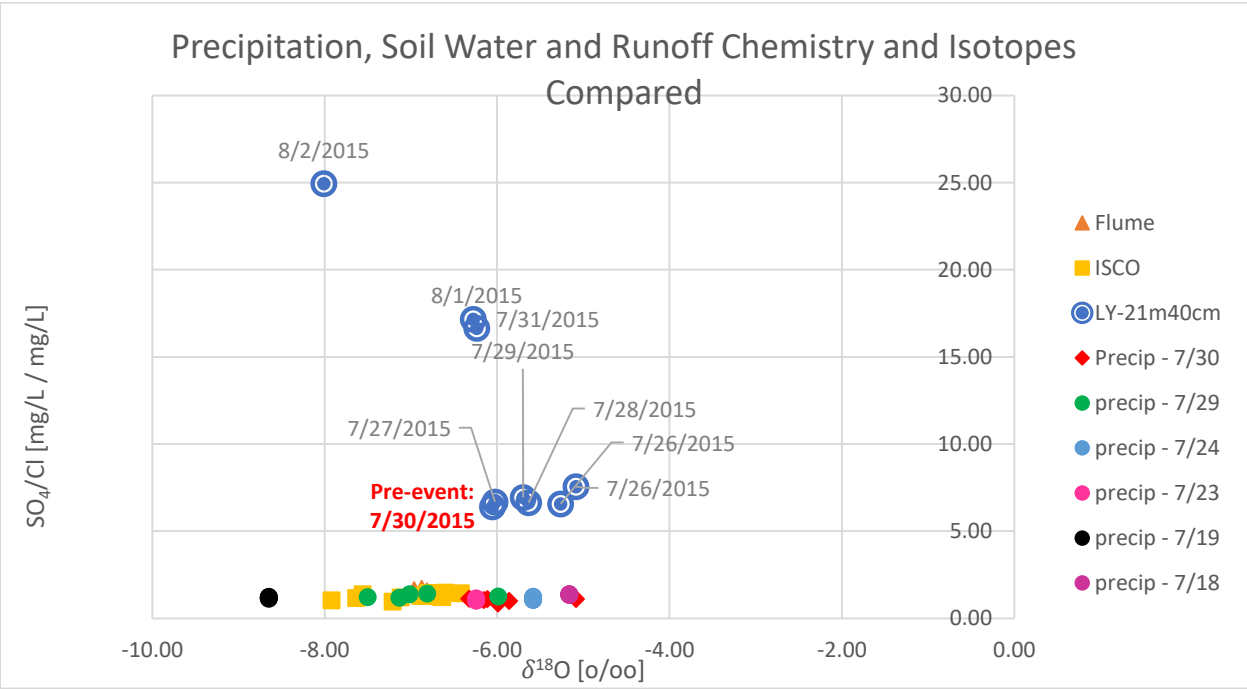

Figure 24: Comparison of precipitation (points), soil water (bullseyes), and runoff (squares and triangles) using the ratio of anions SO_4 and Cl, and $\delta^{18}O$

Table 1: KINEROS2 output from 7/30/2015 runoff at Lucky Hills Flume 103

ID	Element Type	Element Area [m^2]	Cumulated Area [m^2]	Inflow [cu m]	Rainfall [cu m]	Outflow [cu m]	Peak Flow [mm/hr]	Total Infiltration [cu m]	Initial Water Content
51	Plane	12517.56	12517.56	0	148.803	3.682	2.799	145.015	0.1245
52	Plane	812.43	812.43	0	9.554	0.566	10.54	8.99	0.1245
53	Plane	2331.72	2331.72	0	27.402	1.575	7.539	25.799	0.1245
11	Plane	1511.16	1511.16	0	17.706	0.284	1.926	17.412	0.1245
12	Plane	772.28	772.28	0	9.161	0.288	5.902	8.872	0.1245
13	Plane	134.7	134.7	0	1.592	0.135	20.486	1.456	0.1245
92	Plane	1940.28	1940.28	0	23.184	0.674	4.792	22.506	0.1245
93	Plane	5525.58	5525.58	0	65.847	2.006	3.206	63.717	0.1245
31	Plane	1610.75	1610.75	0	19.44	0.408	2.999	18.981	0.1245
32	Plane	1481.49	1481.49	0	17.974	0.906	7.038	17.04	0.1245
33	Plane	392.94	392.94	0	4.93	0.282	16.552	4.647	0.1245
102	Plane	182.9	182.9	0	2.291	0.21	21.135	2.08	0.1245
103	Plane	4897	4897	0	61.064	1.901	3.187	59.087	0.1245
71	Plane	225.99	225.99	0	2.772	0.155	8.495	2.613	0.1245
72	Plane	1122.92	1122.92	0	14.054	1.047	17.541	13	0.1245
73	Plane	1139.68	1139.68	0	14.274	1.025	16.831	13.242	0.1245
112	Plane	14.06	14.06	0	0.186	0.022	20.92	0.165	0.1245
113	Plane	11.1	11.1	0	0.147	0.017	20.424	0.13	0.1245
54	Channel	83.5	15745.21	5.871	1.043	5.705	3.661	1.14	0.1245
14	Channel	41.5	2459.64	0.733	0.521	0.682	3.134	0.527	0.1245
94	Channel	148.23	25818.93	9.14	1.972	8.691	3.09	2.357	0.1245
34	Channel	53.13	3538.31	1.644	0.706	1.554	4.932	0.754	0.1245
104	Channel	141.62	34578.77	12.446	1.974	11.946	3.203	2.398	0.1245
74	Channel	61.58	2550.17	2.282	0.817	2.2	12.484	0.881	0.1245
114	Channel	18.55	37172.64	14.155	0.26	14.084	3.601	0.32	0.1245

Table 2: Method to weigh precipitation by rain gauge importance (with respect to their Theissen Polygon's contributions to the total runoff). KINEROS2 elements and their runoff outflows were partitioned into their respective Thiessen Polygons, allowing the contribution of each element-Thiessen polygon pair to the runoff to be found.

			Element Area Distribution					**Rain Gauge Contribution to Total Runoff**				
			(a)	(b)	(c)	(d)	(e)	(a)	(b)	(c)	(d)	(e)
Plane	Outflow [cu m]	% of total RO	RG-083	RG-386	RG-384	RG-P105	RG-301	RG-083	RG-386	RG-384	RG-P105	RG-301
51	3.682	24.3	100%					24.25%				
52	0.566	3.7	100%					3.73%				
53	1.575	10.4	100%					10.37%				
11	0.284	1.9	100%					1.87%				
12	0.288	1.9	100%					1.90%				
13	0.135	0.9	100%					0.89%				
92	0.674	4.4	78%	22%				3.48%	0.96%			
93	2.006	13.2	87%	13%				11.55%	1.66%			
31	0.408	2.7	18%	82%				0.48%	2.21%			
32	0.906	6.0		93%		7%			5.56%		0.41%	
33	0.282	1.9		100%					1.86%			
102	0.21	1.4		100%					1.38%			
103	1.901	12.5	3%	58%	39%			0.35%	7.32%	4.85%		
71	0.155	1.0		58%		42%			0.60%		0.42%	
72	1.047	6.9		97%		3%			6.67%		0.23%	
73	1.025	6.8		97%		3%			6.54%		0.21%	
112	0.022	0.1		100%					0.14%			
113	0.017	0.1	100%					0.11%				
								Rain Gauge Weights				
								58.98 %	**34.90 %**	**4.85 %**	**1.27 %**	*0%*

Table 3: Description of runoff intensity and amount on 7/30/2015 at Lucky Hills Flume 103

Flume	Date	Start Time [min]	Elapsed Time [min]	Runoff Rate [mm/hr]	Accumulated Volume [mm]
103	7/30/2015	17:04	0	0.000	0.000
103	7/30/2015	17:04	0.25	0.003	0.000
103	7/30/2015	17:04	2.25	0.003	0.000
103	7/30/2015	17:04	3.25	0.013	0.000
103	7/30/2015	17:04	4.25	0.013	0.000
103	7/30/2015	17:04	5.25	0.397	0.004
103	7/30/2015	17:04	6.25	1.667	0.021
103	7/30/2015	17:04	7.25	2.403	0.055
103	7/30/2015	17:04	8.25	2.682	0.097
103	7/30/2015	17:04	9.25	2.951	0.144
103	7/30/2015	17:04	10.25	3.232	0.196
103	7/30/2015	17:04	11.25	3.526	0.252
103	7/30/2015	17:04	14.25	3.526	0.428
103	7/30/2015	17:04	15.25	3.232	0.485
103	7/30/2015	17:04	16.25	2.951	0.536
103	7/30/2015	17:04	17.25	2.403	0.581
103	7/30/2015	17:04	18.25	1.896	0.617
103	7/30/2015	17:04	19.25	1.667	0.646
103	7/30/2015	17:04	20.25	1.077	0.669
103	7/30/2015	17:04	21.25	0.761	0.685
103	7/30/2015	17:04	22.25	0.626	0.696
103	7/30/2015	17:04	23.25	0.504	0.706
103	7/30/2015	17:04	24.25	0.397	0.713
103	7/30/2015	17:04	25.25	0.305	0.719
103	7/30/2015	17:04	26.25	0.159	0.723
103	7/30/2015	17:04	27.25	0.105	0.725
103	7/30/2015	17:04	28.25	0.064	0.726
103	7/30/2015	17:04	29.25	0.033	0.727
103	7/30/2015	17:04	30.25	0.013	0.728
103	7/30/2015	17:04	31.25	0.013	0.728
103	7/30/2015	17:04	32.25	0.003	0.728
103	7/30/2015	17:04	32.5	0.000	0.728

APPENDIX A: ISOTOPE DATASETS FOR PRECIPITATION, SOIL WATER AND RUNOFF

Table 4: Isotope dataset for precipitation at Lucky Hills

Sample Code	Sample Site	Event Start Date	Accum Precip [cm]	Mineral Oil? (Y=1, N=0)	Collect Date	Collect Time	δD [‰]	δD stdev	$\delta^{18}O$ [‰]	$\delta^{18}O$ stdev
LH-P004	RG-083_R	6/25/2015	0.064	0	6/26/2015	12:13	-6.134	2.81E-01	0.125	1.76E-02
LH-P006	RG-083_C1	6/25/2015	0.064	1	6/26/2015	12:20	-36.962	3.34E-01	-4.589	3.51E-02
LH-P013	RG-083_R	6/26/2015	0.292	0	6/27/2015	7:55	-17.402	5.20E-01	-2.158	2.07E-01
LH-P015	RG-083_C1	6/26/2015	0.292	1	6/27/2015	8:00	-19.959	2.09E-01	-1.846	1.90E-01
LH-P023	RG-083_R	6/27/2015	0.064	0	6/28/2015	7:14	14.032	6.01E-01	4.527	1.43E-01
LH-P025	RG-083_C1	6/27/2015	0.064	1	6/28/2015	7:23	-2.872	3.30E-01	0.886	6.28E-03
LH-P033	RG-083_R	7/3/2015	0.597	0	7/8/2015	14:27	26.178	4.22E-01	5.677	4.94E-02
LH-P035	RG-083_C1	7/3/2015	0.597	1	7/8/2015	14:32	-9.586	1.23E-01	-0.613	2.93E-01
LH-P043	RG-083_R	7/12/2015	0.025	0	7/13/2015	9:25	26.408	9.90E-02	9.332	3.16E-01
LH-P045	RG-083_C1	7/12/2015	0.025	1	7/13/2015	9:32	4.231	2.88E-01	0.141	2.49E-01
LH-P052	RG-083_R	7/14/2015	0.051	0	7/15/2015	10:00	-27.318	4.99E-01	-2.437	2.55E-01
LH-P054	RG-083_C1	7/14/2015	0.051	1	7/15/2015	10:05	-36.475	1.76E-01	0.603	2.32E-01
LH-P062	RG-083_R	7/16/2015	0.368	0	7/17/2015	11:31	-27.049	0.00E+00	-3.381	0.00E+00
LH-P064	RG-083_C1	7/16/2015	0.368	1	7/17/2015	11:36	-29.625	0.00E+00	-3.011	0.00E+00
LH-P074	RG-083_R	7/18/2015	0.318	0	7/18/2015	18:56	-25.571	1.07E-01	-4.038	1.64E-01
LH-P076	RG-083_C1	7/18/2015	0.318	1	7/18/2015	19:01	-27.656	1.85E-01	-5.163	1.28E-01
LH-P084	RG-083_R	7/19/2015	0.305	0	7/19/2015	18:13	-50.082	2.48E-01	-6.458	1.46E-01
LH-P086	RG-083_C1	7/19/2015	0.305	1	7/19/2015	18:18	-52.071	5.83E-01	-8.647	2.83E-01
LH-P094	RG-083_R	7/23/2015	0.699	0	7/24/2015	13:49	-37.859	2.51E-01	-4.710	1.18E-01
LH-P096	RG-083_C1	7/23/2015	0.699	1	7/24/2015	13:52	-45.172	4.79E-01	-6.244	1.41E-01
LH-P104	RG-083_R	7/24/2015	0.762	0	7/25/2015	17:23	-30.523	9.99E-02	-3.685	1.73E-01
LH-P106	RG-083_C1	7/24/2015	0.762	1	7/25/2015	17:27	-42.262	5.91E-01	-5.580	1.13E-01
LH-P109	RG-386_C	7/29/2015	n/a	1	7/30/2015	12:10	-51.513	1.32E-01	-7.135	7.65E-02
LH-P110	RG-P105_NR	7/29/2015	n/a	1	7/30/2015	12:15	-53.635	3.96E-01	-7.501	4.56E-02
LH-P111	RG-P105_C	7/29/2015	n/a	1	7/30/2015	12:17	-54.226	5.28E-01	-8.512	4.81E-02
LH-P112	RG-384_NR	7/29/2015	0.025	1	7/30/2015	12:24	-44.331	4.94E-01	-5.988	3.57E-02

LH-P113	RG-384_C	7/29/2015	0.025	1	7/30/2015	12:26	-45.282	9.77E-02	-5.860	1.29E-01
LH-P114	RG-083_R	7/29/2015	0.089	0	7/30/2015	12:35	-19.456	3.08E-01	1.095	1.76E-01
LH-P115	RG-083_NR	7/29/2015	0.089	0	7/30/2015	12:38	-26.135	3.71E-01	-2.227	8.39E-02
LH-P116	RG-083_C1	7/29/2015	0.089	1	7/30/2015	12:41	-50.709	2.49E-01	-7.218	1.44E-01
LH-P117	RG-083_C2	7/29/2015	0.089	1	7/30/2015	12:44	-51.552	6.26E-01	-7.016	3.42E-02
LH-P118	RG-301_C	7/29/2015	n/a	1	7/30/2015	12:52	-49.810	3.08E-01	-6.812	6.29E-02
LH-P119	RG-386_C	7/30/2015	n/a	1	7/31/2015	8:14	-44.152	3.63E-01	-6.112	7.41E-02
LH-P120	RG-P105_NR	7/30/2015	n/a	1	7/31/2015	8:18	-44.954	4.21E-01	-6.325	1.30E-01
LH-P121	RG-P105_C	7/30/2015	n/a	1	7/31/2015	8:25	-44.952	4.90E-01	-5.977	5.47E-02
LH-P122	RG-384_NR	7/30/2015	1.334	1	7/31/2015	9:52	-46.032	6.06E-01	-5.086	1.82E-01
LH-P123	RG-384_C	7/30/2015	1.334	1	7/31/2015	9:54	-45.927	0.00E+00	-5.861	0.00E+00
LH-P124	RG-083_R	7/30/2015	1.232	0	7/31/2015	10:07	-41.184	5.53E-01	-5.563	1.32E-02
LH-P125	RG-083_NR	7/30/2015	1.232	0	7/31/2015	10:11	-43.918	4.58E-01	-5.085	8.39E-02
LH-P126	RG-083_C1	7/30/2015	1.232	1	7/31/2015	n/a	-44.588	1.00E+00	-5.991	1.45E-01
LH-P127	RG-083_C2	7/30/2015	1.232	1	7/31/2015	n/a	-43.992	1.82E-01	-6.155	3.53E-02
LH-P129	RG-386_C	7/31/2015	n/a	1	8/1/2015	11:55	-23.494	3.19E-01	-3.822	8.66E-02
LH-P130	RG-P105_NR	7/31/2015	n/a	1	8/1/2015	12:00	-25.760	6.48E-01	-4.412	2.52E-01
LH-P131	RG-P105_C	7/31/2015	n/a	1	8/1/2015	12:02	-26.169	4.34E-01	-4.954	2.61E-01
LH-P132	RG-384_NR	7/31/2015	0.254	1	8/1/2015	12:16	-24.287	4.99E-02	-4.310	2.48E-01
LH-P133	RG-384_C	7/31/2015	0.254	1	8/1/2015	12:18	-23.537	8.00E-01	-4.447	2.58E-01
LH-P135	RG-083_NR	7/31/2015	0.241	0	8/1/2015	12:25	-17.038	6.55E-01	-2.864	5.09E-02
LH-P136	RG-083_C1	7/31/2015	0.241	1	8/1/2015	12:26	-22.542	2.24E-01	-5.436	1.11E-01
LH-P137	RG-083_C2	7/31/2015	0.241	1	8/1/2015	12:28	-23.181	4.47E-01	-3.843	8.27E-02
LH-P138	RG-301_C	7/31/2015	n/a	1	8/1/2015	12:35	-23.589	3.91E-01	-4.595	1.10E-01
LH-P143	RG-083_R	8/7/2015	0.203	0	8/8/2015	10:07	-0.563	5.96E-01	14.019	2.02E-01
LH-P148	RG-386_C	8/9/2015	n/a	1	8/10/2015	11:48	-18.459	3.39E-01	-3.589	1.02E-01
LH-P149	RG-P105_NR	8/9/2015	n/a	1	8/10/2015	11:52	-9.521	6.07E-02	-1.052	6.99E-02
LH-P150	RG-P105_C	8/9/2015	n/a	1	8/10/2015	11:57	-16.636	6.81E-01	-2.006	2.91E-01
LH-P152	RG-384_C	8/9/2015	0.025	1	8/10/2015	12:11	-12.554	4.17E-01	-1.858	1.61E-01
LH-P154	RG-083_NR	8/9/2015	0.051	0	8/10/2015	12:19	7.604	4.90E-01	2.088	2.54E-01

LH-P155	RG-083_C1	8/9/2015	0.051	1	8/10/2015	12:22	-14.313	0.00E+00	-2.397	0.00E+00
LH-P156	RG-083_C2	8/9/2015	0.051	1	8/10/2015	12:26	-11.631	8.80E-01	-1.288	2.45E-01
LH-P162	RG-083_R	8/11/2015	0.953	0	8/11/2015	10:44	-22.434	1.09E-01	-4.725	8.46E-02
LH-P163	RG-083_C1	8/11/2015	0.953	1	8/11/2015	10:45	-21.460	5.72E-01	-4.711	6.83E-02
LH-P172	RG-083_R	8/11/2015	0.254	0	8/12/2015	11:11	21.738	6.31E-01	3.936	1.70E-01
LH-P173	RG-083_C1	8/11/2015	0.254	1	8/12/2015	11:13	9.946	9.23E-01	2.254	1.15E-01
LH-P186	RG-083_R	8/16/2015	0.127	0	8/17/2015	9:03	28.208	1.83E-01	3.925	1.25E-01
LH-P188	RG-083_C1	8/16/2015	0.127	1	8/17/2015	9:08	24.502	6.51E-01	3.007	1.11E-01
LH-P196	RG-083_R	8/22/2015	0.330	0	8/23/2015	12:26	-11.947	6.78E-01	-0.231	1.09E-01
LH-P198	RG-083_C1	8/22/2015	0.330	1	8/23/2015	12:30	-32.068	4.24E-01	-4.815	1.75E-01
LH-P206	RG-083_R	8/25/2015	0.318	0	8/26/2015	10:15	5.804	5.69E-01	0.571	3.25E-01
LH-P208	RG-083_C1	8/25/2015	0.318	1	8/26/2015	10:18	-12.652	5.16E-01	-2.953	7.73E-02
LH-P211	RG-386_C	8/26/2015	n/a	1	8/28/2015	14:17	6.057	7.93E-01	0.733	8.94E-02
LH-P212	RG-P105_NR	8/26/2015	n/a	1	8/28/2015	14:19	5.060	2.11E-01	0.573	1.93E-01
LH-P213	RG-P105_C	8/26/2015	n/a	1	8/28/2015	14:23	5.967	4.15E-01	1.013	1.14E-01
LH-P214	RG-384_NR	8/26/2015	0.622	1	8/28/2015	14:33	5.222	3.97E-01	1.532	1.12E-01
LH-P215	RG-384_C	8/26/2015	0.622	1	8/28/2015	14:34	6.290	3.41E-01	2.115	1.46E-01
LH-P216	RG-083_R	8/26/2015	0.686	0	8/28/2015	14:40	30.093	4.90E-01	3.782	2.20E-01
LH-P217	RG-083_NR	8/26/2015	0.686	0	8/28/2015	14:42	19.977	4.19E-01	4.854	6.67E-02
LH-P218	RG-083_C1	8/26/2015	0.686	1	8/28/2015	14:43	6.956	5.66E-01	0.605	2.45E-01
LH-P219	RG-083_C2	8/26/2015	0.686	1	8/28/2015	14:45	5.239	2.65E-01	1.120	3.18E-02
LH-P220	RG-301_C	8/26/2015	n/a	1	8/28/2015	14:56	6.409	5.98E-01	1.606	7.05E-03
LH-P235	RG-083_NR	9/3/2015	0.394	0	9/4/2015	10:38	4.106	4.38E-01	-1.894	1.00E-01
LH-P244	RG-083_R	9/4/2015	1.080	0	9/5/2015	14:00	-53.747	4.25E-01	-7.515	7.84E-02
LH-P246	RG-083_C1	9/4/2015	1.080	1	9/5/2015	14:04	-54.743	4.55E-01	-7.845	1.10E-01

Table 5: Isotope dataset for precipitation at Kendall

Sample Code	Sample Site	Event Start Date	Accum Precip [in]	Mineral Oil? (Y=1, N=0)	Collect Date	Collect Time	δD [‰]	δD stdev	$\delta^{18}O$ [‰]	$\delta^{18}O$ stdev
KN-P089	RG-109_C	7/29/2015	n/a	1	7/30/2015	9:20	-61.457	8.42E-01	-7.608	1.91E-01
KN-P090	RG-082_R	7/29/2015	0.025	0	7/30/2015	9:40	-38.980	3.10E-01	-2.386	1.52E-01
KN-P091	RG-082_NR	7/29/2015	0.025	0	7/30/2015	9:43	-41.301	8.28E-01	-4.653	5.21E-02
KN-P092	RG-082_C1	7/29/2015	0.025	1	7/30/2015	9:46	-58.365	4.39E-01	-6.974	2.00E-01
KN-P093	RG-082_C2	7/29/2015	0.025	1	7/30/2015	9:49	-58.873	4.84E-01	-8.321	1.79E-01
KN-P094	RG-061_NR	7/29/2015	<0.01	1	7/30/2015	9:59	-12.677	3.69E-01	3.735	9.91E-02
KN-P095	RG-061_C	7/29/2015	<0.01	1	7/30/2015	10:01	-40.251	6.48E-01	-2.911	1.15E-01
KN-P096	RG-060_NR	7/29/2015	<0.01	1	7/30/2015	10:14	-20.939	2.37E-01	2.181	8.99E-02
KN-P097	RG-060_C	7/29/2015	<0.01	1	7/30/2015	10:17	-36.196	2.91E-01	-2.118	8.99E-02
KN-P107	RG-109_C	8/9/2015	n/a	1	8/10/2015	9:38	-15.447	4.26E-01	-2.618	7.62E-03
KN-P110	RG-082_C1	8/9/2015	0.076	1	8/10/2015	9:50	-15.546	3.70E-01	-1.247	3.58E-01
KN-P112	RG-061_NR	8/9/2015	0.051	1	8/10/2015	10:07	-14.740	3.77E-01	-2.070	7.66E-02
KN-P114	RG-060_NR	8/9/2015	0.051	1	8/10/2015	10:22	-15.919	2.59E-01	-2.171	6.40E-02
KN-P141	RG-109_C	8/27/2015	n/a	1	8/28/2015	12:15	-4.465	2.26E-01	-1.431	8.24E-02
KN-P144	RG-082_C1	8/27/2015	1.270	1	8/28/2015	12:27	-5.208	2.88E-01	-1.762	1.17E-01
KN-P146	RG-061_NR	8/27/2015	1.473	1	8/28/2015	12:43	-5.921	5.24E-01	-2.230	2.14E-01
KN-P148	RG-060_NR	8/27/2015	1.511	1	8/28/2015	12:59	-9.456	1.76E-01	-2.991	1.43E-01

Table 6: Isotope dataset for runoff at Lucky Hills

Sample Code	Type	Sample Site	Collect Date	Collect Time	δD [‰]	δD stdev	$\delta^{18}O$ [‰]	$\delta^{18}O$ stdev
LH-I001	ISCO Runoff	LH-ISCO	7/30/2015	16:55	-42.310	3.91E-01	-7.920	3.18E-02
LH-I002	ISCO Runoff	LH-ISCO	7/30/2015	16:56	-41.886	5.14E-01	-7.636	1.06E-01
LH-I003	ISCO Runoff	LH-ISCO	7/30/2015	16:57	-44.571	0.00E+00	-6.637	0.00E+00
LH-I004	ISCO Runoff	LH-ISCO	7/30/2015	16:58	-45.284	1.27E-01	-6.685	8.11E-02
LH-I005	ISCO Runoff	LH-ISCO	7/30/2015	16:59	-45.054	3.38E-01	-7.119	2.75E-02
LH-I006	ISCO Runoff	LH-ISCO	7/30/2015	17:00	-48.910	4.44E-01	-7.212	1.39E-01
LH-I007	ISCO Runoff	LH-ISCO	7/30/2015	17:01	-48.046	4.12E-01	-6.660	8.47E-02
LH-I008	ISCO Runoff	LH-ISCO	7/30/2015	17:02	-47.849	2.17E-01	-6.690	5.35E-02
LH-I009	ISCO Runoff	LH-ISCO	7/30/2015	17:03	-46.873	3.13E-01	-6.800	6.90E-02
LH-I010	ISCO Runoff	LH-ISCO	7/30/2015	17:04	-45.930	2.38E-01	-6.600	5.67E-02
LH-I011	ISCO Runoff	LH-ISCO	7/30/2015	17:05	-46.890	2.41E-01	-6.420	4.58E-02
LH-I012	ISCO Runoff	LH-ISCO	7/30/2015	17:06	-48.467	3.11E-01	-6.683	1.18E-01
LH-I013	ISCO Runoff	LH-ISCO	7/30/2015	17:07	-47.545	1.96E-01	-6.805	1.52E-01
LH-I014	ISCO Runoff	LH-ISCO	7/30/2015	17:08	-48.229	2.26E-01	-7.559	9.73E-02
LH-I015	ISCO Runoff	LH-ISCO	7/30/2015	17:09	-46.345	0.00E+00	-6.827	0.00E+00
LH-I016	ISCO Runoff	LH-ISCO	7/30/2015	17:10	-46.110	0.00E+00	-6.857	0.00E+00
LH-I017	ISCO Runoff	LH-ISCO	7/30/2015	17:11	-46.702	2.59E-01	-6.893	5.61E-02
LH-F001	Flume Runoff	LH-F103	7/30/2015	17:12	-42.908	1.11E-01	-6.962	6.84E-02
LH-F002	Flume Runoff	LH-F103	7/30/2015	17:15	-46.046	1.44E-01	-6.872	1.52E-01
LH-F003	Flume Runoff	LH-F103	7/30/2015	17:18	-46.730	2.44E-01	-6.814	8.08E-02
LH-F004	Flume Runoff	LH-F103	7/30/2015	17:21	-45.035	9.08E-03	-6.642	3.88E-02

Table 7: Isotope dataset for soil water at Lucky Hills

Sample Code	Sample Site	Collect Date	Collect Time	δD [‰]	δD stdev	$\delta^{18}O$ [‰]	$\delta^{18}O$ stdev
LH-L009	LH-LY-9m40cm	7/31/2015	8:50	-47.795	1.94E-01	-5.298	6.08E-02
LH-L011	LH-LY-9m40cm	8/1/2015	12:09	-48.435	7.04E-01	-4.944	8.41E-02
LH-L018	LH-LY-9m40cm	8/2/2015	8:04	-48.430	5.08E-01	-5.058	2.35E-01
LH-L021	LH-LY-9m40cm	8/4/2015	16:53	-48.434	3.95E-01	-5.620	9.71E-02
LH-L025	LH-LY-9m40cm	8/5/2015	8:00	-48.368	4.82E-01	-4.533	1.43E-01
LH-L029	LH-LY-9m40cm	8/6/2015	11:55	-48.633	4.30E-01	-6.388	1.62E-01
LH-L037	LH-LY-9m40cm	8/11/2015	11:00	-42.988	4.37E-01	-4.644	3.55E-01
LH-L040	LH-LY-9m40cm	8/12/2015	11:33	-45.135	6.03E-01	-6.790	2.74E-01
LH-L043	LH-LY-9m40cm	8/13/2015	12:10	-43.291	3.83E-01	-5.684	1.50E-01
LH-L045	LH-LY-9m40cm	8/14/2015	13:22	-41.033	1.11E-01	-5.405	9.84E-02
LH-L047	LH-LY-9m40cm	8/15/2015	12:28	-36.906	2.86E-01	-5.354	9.63E-02
LH-L010	LH-LY-9m60cm	7/31/2015	8:55	-77.252	2.57E-01	-9.617	1.75E-01
LH-L012	LH-LY-9m60cm	8/1/2015	12:11	-71.588	1.54E-01	-8.458	2.33E-01
LH-L017	LH-LY-9m60cm	8/2/2015	8:02	-69.452	0.00E+00	-8.223	0.00E+00
LH-L022	LH-LY-9m60cm	8/4/2015	16:55	-66.118	1.95E-01	-8.010	1.54E-01
LH-L026	LH-LY-9m60cm	8/5/2015	8:02				
LH-L001	LH-LY-21m40cm	7/26/2015	12:50	-45.148	1.59E-01	-5.261	1.13E-01
LH-L002	LH-LY-21m40cm	7/26/2015	15:50	-44.573	3.16E-01	-5.086	3.84E-02
LH-L003	LH-LY-21m40cm	7/27/2015	13:25	-47.126	4.55E-01	-6.024	1.50E-01
LH-L004	LH-LY-21m40cm	7/28/2015	8:25	-44.379	4.94E-01	-5.635	4.54E-02
LH-L005	LH-LY-21m40cm	7/29/2015	8:30	-45.231	2.18E-01	-5.695	8.64E-02
LH-L006	LH-LY-21m40cm	7/30/2015	13:00	-47.794	5.44E-01	-6.054	9.18E-02
LH-L007	LH-LY-21m40cm	7/31/2015	8:40	-44.932	2.25E-01	-6.275	8.09E-02
LH-L013	LH-LY-21m40cm	8/1/2015	12:14	-45.987	0.00E+00	-6.236	0.00E+00
LH-L015	LH-LY-21m40cm	8/2/2015	7:52	-44.856	2.27E-01	-8.009	1.72E-01
LH-L019	LH-LY-21m40cm	8/4/2015	16:48	-44.995	2.70E-01	-5.367	2.34E-01

LH-L023	LH-LY-21m40cm	8/5/2015	7:55	-45.025	2.62E-01	-8.364	1.20E-01
LH-L027	LH-LY-21m40cm	8/6/2015	11:50	-45.655	3.73E-01	-6.327	1.57E-01
LH-L030	LH-LY-21m40cm	8/7/2015	11:55	-45.106	4.13E-01	-5.574	1.79E-01
LH-L032	LH-LY-21m40cm	8/8/2015	10:23	-45.970	0.00E+00	-6.686	0.00E+00
LH-L034	LH-LY-21m40cm	8/9/2015	12:25	-45.082	5.46E-01	-6.074	7.35E-02
LH-L035	LH-LY-21m40cm	8/10/2015	12:35	-43.802	7.07E-01	-4.927	3.47E-01
LH-L036	LH-LY-21m40cm	8/11/2015	10:57	-31.717	5.61E-01	-5.522	1.60E-01
LH-L038	LH-LY-21m40cm	8/12/2015	11:25	-32.077	7.25E-01	-5.754	7.97E-02
LH-L041	LH-LY-21m40cm	8/13/2015	12:04	-28.537	7.95E-02	-4.689	1.10E-01
LH-L044	LH-LY-21m40cm	8/14/2015	13:20				
LH-L046	LH-LY-21m40cm	8/15/2015	12:22				
LH-L048	LH-LY-21m40cm	8/16/2015	9:00	-26.309	1.66E-01	-4.518	3.43E-01
LH-L049	LH-LY-21m40cm	8/17/2015	8:40	-24.887	6.85E-01	-1.855	2.48E-01
LH-L050	LH-LY-21m40cm	9/5/2015	13:50	-29.387	2.96E-01	-3.977	3.15E-01
LH-L008	LH-LY-21m60cm	7/31/2015	8:45	-70.077	4.83E-01	-8.525	2.12E-02
LH-L014	LH-LY-21m60cm	8/1/2015	12:16	-66.105	1.50E-01	-7.574	1.83E-01
LH-L016	LH-LY-21m60cm	8/2/2015	7:54	-63.568	5.08E-01	-10.873	4.01E-02
LH-L020	LH-LY-21m60cm	8/4/2015	16:50	-62.559	2.49E-01	-6.712	2.86E-01
LH-L024	LH-LY-21m60cm	8/5/2015	7:57	-59.864	4.48E-01	-7.181	2.51E-01
LH-L028	LH-LY-21m60cm	8/6/2015	11:52	-63.910	3.93E-01	-7.431	9.36E-02
LH-L031	LH-LY-21m60cm	8/7/2015	11:57	-60.587	0.00E+00	-6.720	0.00E+00
LH-L033	LH-LY-21m60cm	8/8/2015	10:25	-56.351	0.00E+00	-6.472	0.00E+00
LH-L039	LH-LY-21m60cm	8/12/2015	11:27	-56.610	4.45E-01	-7.595	4.28E-02
LH-L042	LH-LY-21m60cm	8/13/2015	12:06	-63.128	2.01E-01	-7.420	1.41E-01

APPENDIX B: SOLUTE TRACER DATASETS FOR PRECIPITATION, SOIL WATER AND RUNOFF AT LUCKY HILLS

Table 8: Solute tracer dataset for precipitation at Lucky Hills

Sample Code	Sample Site	Event Start Date	Chloride [mg/L]	Sulfate [mg/L]
LH-P059	RG-301_C	7/16/2015	1.867	3.252
LH-P060	RG-384_NR	7/16/2015	1.859	3.397
LH-P065	RG-083_C2	7/16/2015	1.822	3.230
LH-P066	RG-386_C	7/16/2015	1.784	3.326
LH-P067	RG-P105_NR	7/16/2015	1.908	3.452
LH-P069	RG-386_C	7/18/2015	1.526	2.123
LH-P070	RG-P105_NR	7/18/2015	1.615	2.261
LH-P072	RG-384_NR	7/18/2015	1.638	2.262
LH-P077	RG-083_C2	7/18/2015	1.595	2.159
LH-P078	RG-301_C	7/18/2015	1.485	2.034
LH-P079	RG-386_C	7/19/2015	1.557	1.905
LH-P080	RG-P105_NR	7/19/2015	1.570	1.835
LH-P082	RG-384_NR	7/19/2015	1.580	1.952
LH-P087	RG-083_C2	7/19/2015	1.549	1.833
LH-P088	RG-301_C	7/19/2015	1.517	1.726
LH-P089	RG-386_C	7/23/2015	1.691	1.726
LH-P090	RG-P105_NR	7/23/2015	1.710	1.977
LH-P092	RG-384_NR	7/23/2015	1.595	1.769
LH-P097	RG-083_C2	7/23/2015	1.749	1.817
LH-P098	RG-301_C	7/23/2015	1.473	1.587
LH-P099	RG-386_C	7/24/2015	1.508	1.591
LH-P100	RG-P105_NR	7/24/2015	1.608	1.990
LH-P102	RG-384_NR	7/24/2015	1.554	1.927
LH-P107	RG-083_C2	7/24/2015	1.515	1.628
LH-P108	RG-301_C	7/24/2015	1.526	1.737
LH-P109	RG-386_C	7/29/2015	3.377	4.002

LH-P110	RG-P105_NR	7/29/2015	3.309	4.033
LH-P112	RG-384_NR	7/29/2015	4.417	5.565
LH-P117	RG-083_C2	7/29/2015	2.832	3.935
LH-P118	RG-301_C	7/29/2015	2.834	4.046
LH-P119	RG-386_C	7/30/2015	2.381	2.637
LH-P120	RG-P105_NR	7/30/2015	2.265	2.548
LH-P121	RG-P105_C	7/30/2015	2.533	2.564
LH-P122	RG-384_NR	7/30/2015	2.133	2.371
LH-P126	RG-083_C1	7/30/2015	3.080	3.096
LH-P127	RG-083_C2	7/30/2015	3.746	3.242
LH-P128	RG-301_C	7/30/2015	2.192	2.342

Table 9: Solute tracer dataset for runoff at Lucky Hills

Sample Code	Type	Sample Site	Collect Date	Collect Time	Chloride [mg/L]	Sulfate [mg/L]
LH-I001	ISCO Runoff	LH-ISCO	7/30/2015	16:55	3.170	3.284
LH-I002	ISCO Runoff	LH-ISCO	7/30/2015	16:56	2.992	3.521
LH-I003	ISCO Runoff	LH-ISCO	7/30/2015	16:57	2.808	3.451
LH-I004	ISCO Runoff	LH-ISCO	7/30/2015	16:58	2.587	3.312
LH-I005	ISCO Runoff	LH-ISCO	7/30/2015	16:59	3.224	3.873
LH-I006	ISCO Runoff	LH-ISCO	7/30/2015	17:00	3.736	3.612
LH-I007	ISCO Runoff	LH-ISCO	7/30/2015	17:01	2.588	3.217
LH-I008	ISCO Runoff	LH-ISCO	7/30/2015	17:02	2.505	3.246
LH-I009	ISCO Runoff	LH-ISCO	7/30/2015	17:03	2.550	3.718
LH-I010	ISCO Runoff	LH-ISCO	7/30/2015	17:04	2.746	4.093
LH-I011	ISCO Runoff	LH-ISCO	7/30/2015	17:05	2.639	3.794
LH-I012	ISCO Runoff	LH-ISCO	7/30/2015	17:06	2.621	3.554
LH-I013	ISCO Runoff	LH-ISCO	7/30/2015	17:07	2.532	3.389
LH-I014	ISCO Runoff	LH-ISCO	7/30/2015	17:08	2.602	3.619
LH-I015	ISCO Runoff	LH-ISCO	7/30/2015	17:09	2.512	3.338
LH-I016	ISCO Runoff	LH-ISCO	7/30/2015	17:10	2.658	3.462
LH-I017	ISCO Runoff	LH-ISCO	7/30/2015	17:11	2.636	3.447
LH-F001	Flume Runoff	LH-F103	7/30/2015	17:12	4.462	7.263
LH-F002	Flume Runoff	LH-F103	7/30/2015	17:15	2.712	4.610
LH-F003	Flume Runoff	LH-F103	7/30/2015	17:18	3.026	4.701
LH-F004	Flume Runoff	LH-F103	7/30/2015	17:21	3.279	4.614

Table 10: Solute tracer dataset for soil water at Lucky Hills

Sample Code	Sample Site	Collect Date	Collect Time	Chloride [mg/L]	Sulfate [mg/L]
LH-L001	LH-LY-21m40cm	7/26/2015	12:50	28.019	183.908
LH-L002	LH-LY-21m40cm	7/26/2015	15:50	34.294	259.487
LH-L003	LH-LY-21m40cm	7/27/2015	13:25	25.241	168.654
LH-L004	LH-LY-21m40cm	7/28/2015	8:25	25.653	170.281
LH-L005	LH-LY-21m40cm	7/29/2015	8:30	23.968	166.338
LH-L006	LH-LY-21m40cm	7/30/2015	13:00	22.246	142.276
LH-L007	LH-LY-21m40cm	7/31/2015	8:40	8.189	140.572
LH-L008	LH-LY-21m60cm	7/31/2015	8:45	165.956	58.240
LH-L009	LH-LY-9m40cm	7/31/2015	8:50	39.588	145.463
LH-L010	LH-LY-9m60cm	7/31/2015	8:55	79.277	48.507
LH-L011	LH-LY-9m40cm	8/1/2015	12:09	21.301	**164.444**
LH-L012	LH-LY-9m60cm	8/1/2015	12:11	70.679	50.461
LH-L013	LH-LY-21m40cm	8/1/2015	12:14	6.586	109.674
LH-L014	LH-LY-21m60cm	8/1/2015	12:16	120.696	45.292
LH-L015	LH-LY-21m40cm	8/2/2015	7:52	4.257	**106.247**
LH-L016	LH-LY-21m60cm	8/2/2015	7:54	**102.779**	42.489
LH-L018	LH-LY-9m40cm	8/2/2015	8:04	18.148	**151.617**
LH-L019	LH-LY-21m40cm	8/4/2015	16:48	4.353	**95.914**
LH-L020	LH-LY-21m60cm	8/4/2015	16:50	97.138	44.688
LH-L021	LH-LY-9m40cm	8/4/2015	16:53	19.508	**141.223**
LH-L022	LH-LY-9m60cm	8/4/2015	16:55	3.857	**89.025**
LH-L024	LH-LY-21m60cm	8/5/2015	7:57	89.657	50.680
LH-L025	LH-LY-9m40cm	8/5/2015	8:00	21.186	129.631
LH-L027	LH-LY-21m40cm	8/6/2015	11:50	4.310	**86.706**
LH-L028	LH-LY-21m60cm	8/6/2015	11:52	**84.558**	40.764
LH-L029	LH-LY-9m40cm	8/6/2015	11:55	22.621	**139.931**

APPENDIX C: ISOTOPE DATASET FOR SOIL SAMPLES AT LUCKY HILLS

Table 11: Isotope dataset for soil samples at Lucky Hills

Sample Code	Sample Site	Collect Date	Collect Time	δD [‰]	$\delta^{18}O$ [‰]
LH-S007	LH-SS-21m05cm	7/24/2015	10:30	3.81	-89.87
LH-S001	LH-SS-21m20cm	7/24/2015	10:30	-0.19	2.24
LH-S022	LH-SS-21m02cm	7/25/2015	16:15	-1.15	24.37
LH-S019	LH-SS-21m40cm	7/25/2015	16:15	-22.13	6.62
LH-S018	LH-SS-21m60cm	7/25/2015	16:15	-14.22	11.57
LH-S033	LH-SS-21m05cm	7/26/2015	12:10	-6.63	9.51
LH-S030	LH-SS-21m40cm	7/26/2015	12:10	-16.80	-3.71
LH-S029	LH-SS-21m60cm	7/26/2015	12:10	-22.76	14.11
LH-S045	LH-SS-21m05cm	7/27/2015	12:30	-11.87	10.34
LH-S042	LH-SS-21m40cm	7/27/2015	12:30	-21.04	-8.45
LH-S041	LH-SS-21m60cm	7/27/2015	12:30	-25.78	-6.45
LH-S057	LH-SS-21m05cm	7/28/2015	7:40	-15.29	-2.33
LH-S053	LH-SS-21m40cm	7/28/2015	7:40	-17.96	-11.79
LH-S054	LH-SS-21m60cm	7/28/2015	7:40	-22.72	18.91
LH-S069	LH-SS-21m05cm	7/29/2015	7:55	-11.64	6.76
LH-S066	LH-SS-21m40cm	7/29/2015	7:55	-28.49	-11.52
LH-S065	LH-SS-21m60cm	7/29/2015	7:55	-43.44	-2.47
LH-S080	LH-SS-21m05cm	7/30/2015	11:15	-22.22	-0.51
LH-S077	LH-SS-21m40cm	7/30/2015	11:15	-23.86	14.77
LH-S092	LH-SS-21m05cm	7/31/2015	7:30	-30.68	9.51
LH-S089	LH-SS-21m40cm	7/31/2015	7:30	-21.49	-6.35
LH-S088	LH-SS-21m60cm	7/31/2015	7:30	-15.79	12.84

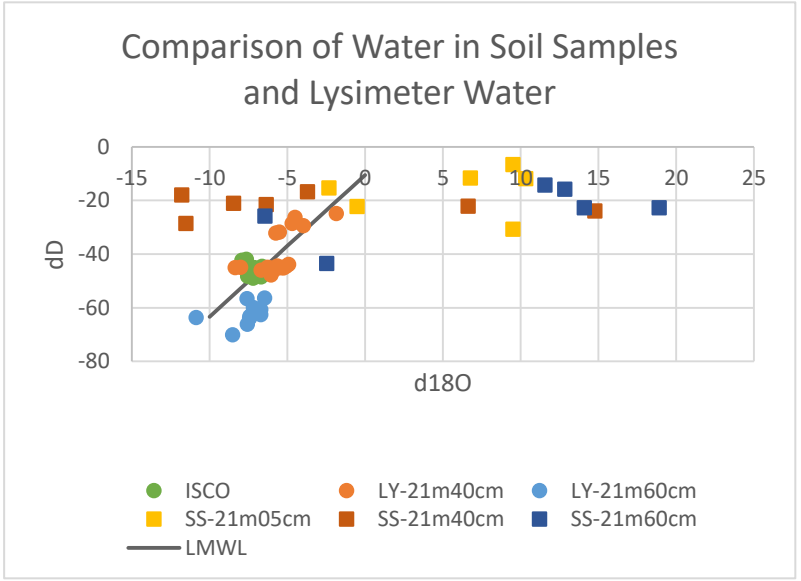

Figure 25: Isotope values of soil samples (squares) compared to the soil water collected by the lysimeters at the same sample location and depths (circles), and runoff (ISCO water). Lysimeters and soil samples are labeled according to their distance from Flume 103 (21 m) and depth (5, 40 or 60 cm)

REFERENCES

Allison, G. B., & Hughes, M. W. (1983). The use of natural tracers as indicators of soil-water movement in a temperate semi-arid region. *Journal of Hydrology*, *60*(1-4), 157-173.

Allison, G. B., Gee, G. W., & Tyler, S. W. (1994). Vadose-zone techniques for estimating groundwater recharge in arid and semiarid regions. *Soil Science Society of America Journal*, *58*(1), 6-14.

Allison, G. B., Stone, W. J., & Hughes, M. W. (1985). Recharge in karst and dune elements of a semi-arid landscape as indicated by natural isotopes and chloride. *Journal of Hydrology*, *76*(1-2), 1-25.

Arnell, N. W. (1999). Climate change and global water resources. *Global environmental change*, *9*, S31-S49.

Arnell, N. W. (2004). Climate change and global water resources: SRES emissions and socio-economic scenarios. *Global environmental change*, *14*(1), 31-52.

Baillie, M. N., Hogan, J. F., Ekwurzel, B., Wahi, A. K., & Eastoe, C. J. (2007). Quantifying water sources to a semiarid riparian ecosystem, San Pedro River, Arizona. *Journal of Geophysical Research: Biogeosciences*, *112*(G3).

Brammer, D. D. (1996). *Hillslope hydrology in a small forested catchment, Maimai, New Zealand* (Order No. 1382126). Available from ProQuest Dissertations & Theses Global. (304265292)

Breckenfeld, D. J., Svetlik, W. A., & McGuire, C. E. (1995). Soil survey of walnut gulch experimental watershed. *Tucson, AZ: USDA Soil Conservation Service*.

Clark, I. D., & Fritz, P. (1997). *Environmental isotopes in hydrogeology*. CRC press.

Dansgaard, W. (1964). Stable isotopes in precipitation. *Tellus*, *16*(4), 436-468.

Eastoe, C. J., & Dettman, D. L. (2016). Isotope amount effects in hydrologic and climate reconstructions of monsoon climates: Implications of some long-term data sets for precipitation. *Chemical Geology*, *430*, 78-89.

Fitzjohn, C., Ternan, J. L., & Williams, A. G. (1998). Soil moisture variability in a semi-arid gully catchment: implications for runoff and erosion control. *Catena*, *32*(1), 55-70.

Gat, J. R. (1980). The isotopes of hydrogen and oxygen in precipitation. In *Handbook of environmental isotope geochemistry. Vol. 1*.

Gehre, M., & Strauch, G. (2003). High-temperature elemental analysis and pyrolysis techniques for stable isotope analysis. *Rapid communications in mass spectrometry*, *17*(13), 1497-1503.

Gochis, D. J., Brito-Castillo, L., & Shuttleworth, W. J. (2006). Hydroclimatology of the North American Monsoon region in northwest Mexico. *Journal of Hydrology*, *316*(1), 53-70.

Goodrich, D. C., Williams, D. G., Unkrich, C. L., Hogan, J. F., Scott, R. L., Hultine, K. R., ... & Miller, S. (2004). Comparison of methods to estimate ephemeral channel recharge, Walnut Gulch, San Pedro River basin, Arizona. *Groundwater recharge in a desert environment: the southwestern United States*, 77-99.

Goodrich, D. C., Keefer, T. O., Unkrich, C. L., Nichols, M. H., Osborn, H. B., Stone, J. J., & Smith, J. R. (2008). Long-term precipitation database, walnut gulch experimental watershed, arizona, united states. *Water Resources Research*, *44*(5), W05S04. doi:10.1029/2006WR005782

Goodrich, D. C., Bums, I. S., Unkrich, C. L., Semmens, D. J., Guertin, D. P., Hernandez, M., ... & Levick, L. R. (2012). KINEROS 2/AGWA: Model use, calibration, and validation. *Transactions of the ASABE*, *55*(4), 1561-1574.

Hrachowitz, M., Savenije, H., Bogaard, T. A., Tetzlaff, D., & Soulsby, C. (2013). What can flux tracking teach us about water age distribution patterns and their temporal dynamics?. *Hydrology and Earth System Sciences*, *17*(2), 533.

Hundecha, Y., & Bárdossy, A. (2004). Modeling of the effect of land use changes on the runoff generation of a river basin through parameter regionalization of a watershed model. *Journal of hydrology*, *292*(1), 281-295.

Ingraham, N. L., Caldwell, E. A., & Verhagen, B. T. (1998). Arid catchments. *Isotope tracers in catchment hydrology. Elsevier, Amsterdam*, 435-465.

Kincaid, D. R., Gardner, J. L., & Schreiber, H. A. (1964). Soil and vegetation parameters affecting infiltration under semiarid conditions. *Land Erosion, Precipitation, Hydrometry, Soil Moisture*, 440-453.

Koch, J. C. (2005). *Quantifying Bulk and Mobile Carbon and Nitrogen in the Dominant Landscapes of the Upper San Pedro River Basin, Arizona*. Unpublished master's thesis, University of Arizona, Tucson, Arizona.

Landon, M. K., Delin, G. N., Komor, S. C., & Regan, C. P. (1999). Comparison of the stable-isotopic composition of soil water collected from suction lysimeters, wick samplers, and cores in a sandy unsaturated zone. *Journal of Hydrology*, *224*(1), 45-54.

Luxmoore, R. J., Jardine, P. M., Wilson, G. V., Jones, J. R., & Zelazny, L. W. (1990). Physical and chemical controls of preferred path flow through a forested hillslope. *Geoderma*, *46*(1-3), 139-154.

Maneta, M., Schnabel, S., & Jetten, V. (2008). Continuous spatially distributed simulation of surface and subsurface hydrological processes in a small semiarid catchment. *Hydrological Processes*, *22*(13), 2196-2214.

McDonnell, J. J., Stewart, M. K., & Owens, I. F. (1991). Effect of catchment-scale subsurface mixing on stream isotopic response. *Water Resources Research, 27*(12), 3065-3073.

McGlynn, B. L., & McDonnell, J. J. (2003). Quantifying the relative contributions of riparian and hillslope zones to catchment runoff. *Water Resources Research, 39*(11).

McGuire, K. J., Weiler, M., & McDonnell, J. J. (2007). Integrating tracer experiments with modeling to assess runoff processes and water transit times. *Advances in Water Resources, 30*(4), 824-837.

Miller, S. N., Semmens, D. J., Goodrich, D. C., Hernandez, M., Miller, R. C., Kepner, W. G., & Guertin, D. P. (2007). The automated geospatial watershed assessment tool. *Environmental Modelling & Software, 22*(3), 365-377.

Nichols, M. H., Stone, J. J., & Nearing, M. A. (2008). Sediment database, walnut gulch experimental watershed, arizona, united states. *Water Resources Research, 44*(5), W05S06. doi:10.1029/2006WR005682

Osborn, H. B., & Reynolds, W. N. (1963). Convective storm patterns in the southwestern United States. *Hydrological Sciences Journal, 8*(3), 71-83.

Pearce, A. J., Stewart, M. K., & Sklash, M. G. (1986). Storm runoff generation in humid headwater catchments: 1. Where does the water come from?. *Water Resources Research, 22*(8), 1263-1272.

Peters, N. E., & Ratcliffe, E. B. (1998). Tracing hydrologic pathways using chloride at the Panola Mountain Research Watershed, Georgia, USA. *Water, Air, and Soil Pollution, 105*(1-2), 263-275.

Pilgrim, D. H., Chapman, T. G., & Doran, D. G. (1988). Problems of rainfall-runoff modelling in arid and semiarid regions. *Hydrological Sciences Journal, 33*(4), 379-400.

Puigdefabregas, J., del Barrio, G., Boer, M. M., Gutierrez, L., & Sole, A. (1998). Differential responses of hillslope and channel elements to rainfall events in a semi-arid area. *Geomorphology, 23*(2), 337-351.

Ragab, R., & Prudhomme, C. (2002). Sw—soil and Water: climate change and water resources management in arid and semi-arid regions: prospective and challenges for the 21st century. *Biosystems engineering, 81*(1), 3-34.

Renard, K. G., Lane, L. J., Simanton, J. R., Emmerich, W. E., Stone, J. J., Weltz, M. A., ... & Yakowitz, D. S. (1993). Agricultural impacts in an arid environment: Walnut Gulch studies. *Hydrological Science and Technology, 9*(1-4), 145-190.

Robertson, F. N. (1989). Arsenic in ground-water under oxidizing conditions, south-west United States. *Environmental geochemistry and Health, 11*(3), 171-185.

Robertson, F. N. (1992). Radiocarbon dating of groundwater in a confined aquifer in southeast Arizona. *Radiocarbon*, *34*(03), 664-676.

Robinson, J. S., & Sivapalan, M. (1995). Catchment-scale runoff generation model by aggregation and similarity analyses. *Hydrological processes*, *9*(5-6), 555-574.

Schaik, N. L. M. B., Bronstert, A., Jong, S. M., Jetten, V. G., Dam, J. C., Ritsema, C. J., & Schnabel, S. (2014). Process-based modelling of a headwater catchment in a semi-arid area: the influence of macropore flow. *Hydrological processes*, *28*(24), 5805-5816.

Scholl, M. A., Ingebritsen, S. E., Janik, C. J., & Kauahikaua, J. P. (1996). Use of precipitation and groundwater isotopes to interpret regional hydrology on a tropical volcanic island: Kilauea volcano area, Hawaii. *Water Resources Research*, *32*(12), 3525-3537.

Scott, R. L., Shuttleworth, W. J., Keefer, T. O., & Warrick, A. W. (2000). Modeling multiyear observations of soil moisture recharge in the semiarid American Southwest. *Water Resources Research*, *36*(8), 2233-2247.

Skirvin, S., Kidwell, M., Biedenbender, S., Henley, J. P., King, D., Collins, C. H., ... & Weltz, M. (2008). Vegetation data, walnut gulch experimental watershed, arizona, united states. Water Resources Research, 44(5), W05S08. doi:10.1029/2006WR005724

Smith, R. E., & Hebbert, R. H. B. (1979). A Monte Carlo analysis of the hydrologic effects of spatial variability of infiltration. *Water Resources Research*, *15*(2), 419-429.

Sprenger, M., Herbstritt, B., & Weiler, M. (2015). Established methods and new opportunities for pore water stable isotope analysis. *Hydrological Processes*, *29*(25), 5174-5192.

Van Schaik, N. L. M. B., Schnabel, S., & Jetten, V. G. (2008). The influence of preferential flow on hillslope hydrology in a semi-arid watershed (in the Spanish Dehesas). *Hydrological processes*, *22*(18), 3844-3855.

Weiler, M., & McDonnell, J. (2004). Virtual experiments: a new approach for improving process conceptualization in hillslope hydrology. *Journal of Hydrology*, *285*(1), 3-18.

Wilson, G. V., Jardine, P. M., Luxmoore, R. J., Zelazny, L. W., Lietzke, D. A., & Todd, D. E. (1991). Hydrogeochemical processes controlling subsurface transport from an upper subcatchment of Walker Branch watershed during storm events. 1. Hydrologic transport processes. *Journal of Hydrology*, *123*(3-4), 297-316.

Wood, W. W., & Sanford, W. E. (1995). Chemical and isotopic methods for quantifying ground-water recharge in a regional, semiarid environment. *Ground Water*, *33*(3), 458-468.

Wright, W. E. (2001). Delta-deuterium and delta-oxygen-18 in mixed conifer systems in the United States southwest: The potential of delta-oxygen-18 in Pinus ponderosa tree rings as a natural environmental recorder.

Yair, A., & Lavee, H. (1985). Runoff generation in arid and semi-arid zones. *Hydrological forecasting/edited by MG Anderson and TP Burt*.